Molecular Mechanism of the Immunomodulatory Drug Halofuginone

Molecular Mechanism of the Immunomodulatory Drug Halofuginone

Brendan W. Wu

A Thesis Submitted to the Faculty of

The Harvard Medical School

in Partial Fulfillment of the Requirements

for the Degree of Master of Medical Sciences in Immunology

Harvard University

Boston, Massachusetts

May, 2016

Thesis Advisor: Dr. Malcolm Whitman Brendan W. Wu

Molecular Mechanism of the Immunomodulatory Drug Halofuginone

Abstract

Cellular sensing of amino acid availability has recently emerged as an important mechanism of immunomodulation. Small molecules that manipulate amino acid metabolism serve as powerful tools for studying these poorly characterized signaling pathways. The compound halofuginone, derived from an herb in traditional Chinese medicine, induces a cellular state of proline starvation by inhibiting the prolyl-tRNA synthetase domain of EPRS. The resulting accumulation of uncharged prolyl-tRNA correlated with inhibition of Th17 differentiation and protection against autoimmune disease. Halofuginone invoked the canonical amino acid starvation response (AAR) by increasing phosphorylation of GCN2 and eIF2α to adapt to nutrient stress. However, knockout of GCN2 failed to fully account for the anti-inflammatory properties of halofuginone and did not rescue Th17 differentiation, suggesting immunomodulation through non-canonical AAR pathways. Since GCN2-independent AAR pathways are better characterized in yeast than in mammals, we identified and investigated their orthologs. Co-immunoprecipitation studies validated the formation of an orthologous human GCN1/RWDD1/DRG2 complex. Knockdown of the adaptor protein RWDD1 in fibroblast-like synoviocytes reduced the ability of halofuginone to suppress *CXCL10* and *MMP-13* expression during TNF-α-induced inflammation. A non-canonical AAR pathway involving GCN1, RWDD1, and DRG2 could expand our understanding of how amino acid metabolism regulates immunity and may reveal new drug targets for immunotherapy.

Table of Contents

Abstract ii

Table of Contents iii

List of Figures iv

List of Tables vi

Acknowledgements vii

Chapter One: Background 1

Schematic Figures 11

Chapter Two: Data and Methods 12

Short Introduction 12

Materials and Methods 13

Results 19

Brief Discussion 27

Figures 28

Chapter Three: Discussion and Perspectives 35

Limitations 37

Future Research 39

Bibliography 41

List of Figures

Figure I. Gcn1-dependent signaling during amino acid starvation in yeast……..11
(**A**) In the canonical amino acid starvation response (AAR) pathway, Gcn1 interacts with Gcn2 on translating ribosomes to detect uncharged tRNAs. Gcn2 phosphorylates eIF2α which activates general control of amino acid metabolism. (**B**) In the non-canonical AAR pathway, Gir2 binds to Gcn1 and Rbg1. Rbg1 hydrolyzes GTP into GDP, but the downstream effects are unclear. *Figure adapted from Wout et al., 2009.*

Figure II. Amino acid metabolism modulates immunity……..……...11
Halofuginone treatment mimics proline starvation by inhibiting EPRS activity and IDO induces tryptophan starvation by catabolizing tryptophan into kynurenine. Both mechanisms lead to the accumulation of uncharged tRNAs, activating the amino acid starvation response (AAR) pathway which modulates the immune system.

Figure 1. Effect of halofuginone on proline utilization for translation……...28
(**A**) Flag-tagged gene blocks were designed for cell-free *in vitro* translation. One gene block contained two pairs of proline residues (Pro) and the other lacked proline completely (NoPro). (**B**) 5 μM halofuginone (HF) was added to the *in vitro* translation reactions. Products were analyzed by anti-Flag western blot. (**C**) After *in vitro* translation, reaction mixtures were digested with benzonase nuclease. (**D**) *In vitro* translation reactions with or without 5 μM halofuginone were supplemented with 5 mM *L*-proline.

Figure 2. Subcellular localization of ribosomes and GCN1-signaling components……...29
(**A**) Cytoplasmic extract of K4 cells was run through a Sepharose 6B column and 24 fractions were collected. The absorbance at 280 nm (A280) was measured for all fractions. The column was calibrated with dextran blue (blue points) and Ponceau S (red points). Fractions were screened for eluted proteins by western blot. L13a: large 60S subunit ribosomal marker. (**B**) K4 cells were treated with 200 nM halofuginone (HF) for 1 hour or untreated (Ø). The cytoplasmic fraction was extracted by digitonin permeabilization buffer (DIG). The endoplasmic reticulum (ER) fraction was sequentially extracted by NP-40 lysis buffer (NP-40). Protein localization was compared by western blot. β-actin: cytoplasmic marker. Calreticulin: ER marker.

Figure 3. GCN1 and the canonical amino acid starvation response……...…30
(**A**) K4 cells were transfected with V5-GCN2 and Flag-GCN1 and were treated with 200 nM halofuginone (HF) for 1 hour. Protein extracts were immunoprecipitated with anti-Flag beads and analyzed by anti-Flag and anti-V5 western blot. (**B-C**) K4 cells were transfected with V5-GCN2, Flag-GCN1, and Flag-GCN2 and were treated with halofuginone or untreated (Ø) as in **A**. Immunoprecipitation and western blot as in **A**. (**D**) Phosphorylation of GCN2 and eIF2α after halofuginone treatment as in **a** was assessed by western blot.

Figure 4. GCN1 and the non-canonical amino acid starvation response……...…31
(**A**) K4 cells were transfected with His-RWDD1 and Flag-GCN1 and were treated with 200 nM halofuginone (HF) for 1 hour. Protein extracts were immunoprecipitated with anti-Flag beads and analyzed by anti-His and anti-Flag western blot. (**B**) K4 cells were transfected with His-RWDD1 and Flag-DRG2 and were treated with halofuginone as in **A**. Immunoprecipitation and western blot as in **A**. Endogenous GCN1 was detected by anti-GCN1 western blot.

Figure 5. Approaches to blocking GCN1-dependent signaling..…….....32
(**A**) GCN2, IMPACT, and RWDD1 were truncated to only their RWD domains. (**B**) K4 cells were transduced with V5-tagged RWD domains or EGFP. Stable expression of RWD domains was determined by anti-V5 western blot. (**C**) K4 cells were transfected with EGFP or RWD domains. Phosphorylation of GCN2 in response to incremental doses of halofuginone (HF) for 1 hour was assessed by western blot. (**D**) K4 cells were transfected with EGFP, full-length His-RWDD1, or full-length IMPACT. Phosphorylation of GCN2 in response to 100 nM halofuginone for 1 hour was assessed by western blot. (**E**) K4 cells were transfected with two guide RNAs (gRNAs) targeting GCN1 for CRISPR-Cas9 gene knockout. GCN1 expression was compared to β-actin expression by western blot.

Figure 6. Blocking the non-canonical amino acid starvation response……..…..33
(**A**) K4 cells were transduced with five shRNAs targeting the *Rwdd1* transcript (682, 683, 684, 685, and 686) or a scrambled (scr) shRNA as a control. RWDD1 expression was compared to β-actin and GAPDH expression by western blot. (**B**) Cell lines from **A** were treated with 100 nM or 200 nM halofuginone for 24 hours and 10 ng/μl TNF-α for 8 hours. Expression of *CXCL10* was measured by qPCR. (**C**) Cell lines were treated as in **B**. Expression of *MMP-13* was measured by qPCR.

Figure 7. Proposed molecular mechanism of halofuginone…….…....34
Halofuginone inhibits EPRS, preventing the charging of prolyl-tRNA. Uncharged tRNA activates GCN1 at the ribosome. GCN1 associates with GCN2 in the canonical amino acid starvation response (AAR) pathway. GCN1 also associates with RWDD1 and DRG2 in the non-canonical AAR pathway. How signaling through RWDD1 and DRG2 leads to immunomodulation remains unclear.

List of Tables

Table 1. Cell Lines……..…..13

Table 2. Plasmids……..14

Table 3. Antibodies……...…15

Table 4. Oligonucleotides……...…….16

Acknowledgements

First and foremost, I would like to express gratitude to my principal investigator Malcolm Whitman who believed in my potential and accepted me into this lab. His valuable guidance and support over these past months have made this thesis possible. Second, I am indebted to the members of the Whitman Lab: Yeon-Jin Kim, Leila Revollo, Mattia Bordoli, Du Feng, Maja Edenius, and Kristen Powers. I extend thanks to Tracy Keller and Chang Yeol-Yeo for providing ideas and tools that helped my project greatly. I would also like to thank the directors of Harvard Medical School's Master of Medical Sciences in Immunology program: Shiv Pillai, Michael Carroll, Kevin Bonham, and Selina Labriola. Last but not least, I would like to express my appreciation to my classmates, friends, parents, and sister for their unwavering support and encouragement throughout my two years at Harvard University.

This work was conducted with support from Students in the Master of Medical Sciences in Immunology program of Harvard Medical School. The content is solely the responsibility of the authors and does not necessarily represent the official views of Harvard University and its affiliated academic health care centers.

Chapter One: Background

Bioactive small molecules are important tools in experimental research and have fueled drug discovery. Nature serves as a vast reservoir of molecules that can bind channels, receptors and ribosomal subunits, intercalate into nucleic acids, block microtubule assembly, and inhibit enzymes to modulate biological functions[1,2]. For thousands of years, herbal preparations from plants have been used as medicine; well-known bioactive components or derivatives include aspirin to reduce fever, morphine to relieve pain, and quinine to treat malaria[3]. Identifying novel compounds and deciphering their molecular mechanisms will aid the development of anti-tumorigenic, anti-bacterial, and anti-inflammatory pharmaceuticals as well as expand our understanding of disease processes.

Origin and Synthesis of Halofuginone

The quinazoline-type alkaloid febrifugine is found in the flowering plant *Dichroa febrifuga*, one of the fifty fundamental herbs in traditional Chinese medicine[4]. For centuries, preparations of its roots and leaves have treated malarial fever in China. In the west, interest in febrifugine heightened in the twentieth century when 600 plant extracts were screened for their anti-malarial properties and *D. febrifuga* extractions exhibited one of the highest potencies[5]. Two stereoisomers with the molecular formula $C_{16}H_{21}O_3N_3$ were chemically isolated from the roots and were later named febrifugine and isofebrifugine[6,7]. The bioactive isomer febrifugine was found to be more effective than the established anti-malarial drug quinine for treating the Chesson strain of *Plasmodium vivax* in early clinical trials[8]. However, patients taking febrifugine

experienced symptoms of gastrointestinal toxicity including vomiting, diarrhea, and liver damage[9,10].

In the attempts to synthesize a less toxic derivative, chemists modified the quinazoline ring, the linker, and the piperidine ring of febrifugine[11,12]. A racemic mixture of febrifugine was half as effective as the natural stereoisomer, suggesting that the absolute configuration of the hydroxyl group and the nitrogen of the piperidine ring had to be preserved[13]. Nucleophilic addition to the quinazoline ring had little influence on anti-malarial activity whereas substitution on the linker region greatly reduced activity. The most effective analog involved halogenation of febrifugine's quinazoline ring with chlorine and bromine, producing the compound named halofuginone[14].

Medicinal Properties of Halofuginone

The therapeutic effects of halofuginone are extraordinarily diverse. The bromide salt of halofuginone is a dietary supplement for farmed chicken and turkeys used in the prevention coccidiosis[15]. The lactate salt of halofuginone is administered orally to lamb, cows, and other cattle to prevent cryptosporidiosis[16]. Halofuginone reduces proliferation of the protozoan parasites *Plasmodium falciparum* and *Plasmodium berghei* in both the asymptomatic liver stage and the symptomatic blood stage of malaria[17]. Unlike quinine which only targets mature stages of the *P. falciparum* lifecycle, halofuginone is equally toxic to all three stages (ring stage, trophozoite, and schizont)[18]. In the past few decades, the benefits of halofuginone have been extended beyond malaria to treating cancer, fibrosis, and autoimmunity[19].

Angiogenesis, the formation of new blood vessels from pre-existing vessels, provides oxygen and nutrients to tumor cells. Inhibiting angiogenesis therefore prevents cancer

progression and metastasis. Halofuginone was shown to reduce the diameter and length of blood vessels in pancreatic tumor xenografts in mice[20]. Halofuginone also inhibited angiogenesis in bladder carcinoma[21], prostate cancer[22], Wilms tumor[23], cutaneous melanoma[24], and colorectal cancer[25]. Notably, progression of von Hippel-Lindau-associated tumors expressing high levels of vascular endothelial growth factor, a strong stimulator of angiogenesis, was significantly slowed by halofuginone[26]. Lung metastasis of hepatocellular carcinoma and bone metastasis of melanoma xenografts were significantly hindered by halofuginone[27,28]. Furthermore, halofuginone induced apoptosis, generated reactive oxygen species, and restricted migration of breast cancer cells[29]. Other mechanisms of anti-carcinogenesis included decreasing endothelial cell MMP-2 expression, basic fibroblast growth factor responsiveness, or fibroblast-to-myofibroblast transition[30]. Because halofuginone does not target mitosis or DNA synthesis like common anti-tumorigenic agents, it has been successfully used in combination chemotherapy for prostate, kidney, and pancreatic cancer[31].

Fibrosis is a pathological condition where excessive deposition of fibrous connective tissue such as collagen and glycosaminoglycan interferes with the architecture or function of the underlying organ. *In vitro*, halofuginone inhibited collagen type 1 synthesis by skin fibroblasts from patients with graft-versus-host disease or scleroderma[32]. *In vivo*, halofuginone diminished collagen synthesis in mice afflicted with chronic graft-versus-host disease[33] and pulmonary and pancreatic fibrosis[34]. In a mouse model of Duchenne muscular dystrophy, halofuginone counteracted the fibrotic changes in skeletal, respiratory, and cardiac muscles by decreasing expression of collagen and smooth muscle actin[35]. The anti-fibrotic properties are not only preventative, but also curative. In rats with established hepatic fibrosis, halofuginone reduced levels of collagen to nearly that of unaffected animals and rescued liver regeneration[36]. When

applied to the skin of mice with scleroderma, halofuginone diminished collagen expression and dermal fibroblast proliferation[37]. Resolution of fibrosis may be partially attributed to halofuginone's ability to upregulate MMP-2, MMP-3, and MMP-13, matrix metalloproteinases that degrade extracellular matrix (ECM) proteins such as collagen[38,39] and to downregulate tissue inhibitor of metalloproteinases-2 (TIMP-2)[40]. Halofuginone also modulated TGF-β signaling by inhibiting phosphorylation of the downstream transcription factor Smad3 while simultaneously elevating expression of the negative regulator Smad7[41,42]. TGF-β is a pro-fibrotic cytokine released by macrophages that induces expression of ECM components and inhibitors of the proteases that degrade the ECM[43].

Halofuginone has also shown promise in treating autoimmune disorders. CD4+ T helper cells differentiate into three subsets (Th1, Th2, and Th17) with distinct cytokine profiles and effector functions[44]. Th17 cells produce the pro-inflammatory cytokines IL-17, IL-17F, and IL-22, and their differentiation is induced by the combination of IL-6 and TGF-β[45]. Dysregulation of Th17 cells is associated with many autoimmune diseases such as rheumatoid arthritis, systemic lupus erythematosus, multiple sclerosis, psoriasis, inflammatory bowel disease and Crohn's disease, type 1 diabetes, and more[46]. In a landmark study, halofuginone specifically inhibited the differentiation of human and mouse naïve T cells into Th17 cells but not Th1 or Th2 cells. Treatment did not affect the induction of RORγt, the master transcription factor of Th17 cells, and did not directly inhibit TGF-β or IL-6 signaling, suggesting a novel mechanism of regulation. *In vivo*, halofuginone protected mice from Th17-associated experimental autoimmune encephalomyelitis[47]. Mice with vulvovaginal candidiasis injected with halofuginone also exhibited suppression of Th17 differentiation with an associated decrease in IL-17 production[48]. In an estrogen-deficient osteoporosis animal model, halofuginone reduced the abundance of

Th17 cells and the amount of bone resorption without impacting osteogenesis[49]. Halofuginone lowered the number of Th17 cells and blocked the formation and activity of osteoclasts in a murine autoimmune arthritis model[50]. Induction of MMP-13, a matrix metalloprotease that degrades articular cartilage in rheumatoid arthritis, by TNF-α was mitigated during halofuginone treatment in fibroblast-like synoviocytes. In rodent models of osteoarthritis, halofuginone suppressed Th17-induced osteoclastic bone resorption by opposing TGF-β signaling[51]. In a mouse orthotopic lung transplant model, halofuginone diminished IL-17A levels and ameliorated chronic lung allograft dysfunction[52]. Taken together, these animal studies support the possibility of using halofuginone as an immunomodulatory drug to treat a broad spectrum of human Th17-associated pathologies.

Molecular Mechanisms of Halofuginone

The ability to alleviate seemingly unrelated disorders ranging from cancer to fibrosis to autoimmunity raises the pressing question of whether halofuginone's actions are attributed to common or separate pathways. The clearest link between fibrosis and Th17 immunity is TGF-β signaling, which halofuginone may suppress by indirectly downregulating Smad3 phosphorylation. A more direct mechanism involves halofuginone physically binding to glutamyl-prolyl-tRNA synthetase (EPRS), an enzyme that charges both glutamyl and prolyl tRNAs with glutamate and proline respectively. Halofuginone specifically associated with the prolyl-tRNA synthetase domain (ProRS) but not the glutamyl tRNA synthetase domain of EPRS. In competitive binding assays, addition of excess proline or febrifugine displaced halofuginone from purified ProRS and suggested that halofuginone bound to a site of EPRS that included, at least partly, the proline-binding pocket. Binding to EPRS was also dependent on an ATP-

induced conformational change of the enzyme active site to accommodate the small molecule. Consistent with exclusive targeting of the ProRS domain, addition of proline but not glutamate rescued Th17 differentiation in the presence of halofuginone[53].

By inhibiting EPRS and preventing charging of prolyl-tRNA, halofuginone treatment mimics proline starvation in cells, leading to the activation of the amino acid starvation response (AAR) pathway. Like the AMP-activated protein kinase (AMPK) and target of rapamycin (TOR) pathways, AAR is a highly conserved stress response in eukaryotes that reprograms cellular metabolism[54,55]. Unlike the TOR pathway which senses amino acid availability directly[56], the AAR pathway is triggered when uncharged tRNAs indirectly accumulate during amino acid depletion. The protein kinase GCN2 is activated by uncharged tRNAs which results in its auto-phosphorylation[57]. The translational activator GCN1 is necessary for GCN2 phosphorylation[58]. Activated GCN2 then phosphorylates the translational initiative factor eIF2α, a strong repressor of the guanine nucleotide exchange factor eIF2B, which results in a global downregulation of cap-dependent translation by impeding formation of the eIF2α-GTP-Met-tRNAi ternary complex[59,60]. At the same time, phosphorylated eIF2α elicits the integrated stress response by stimulating the translation of a subset of mRNAs that are involved in adaptation to stress. One target, the transcription factor ATF4, increases the expression of another transcription factor known as C/EBP homologous protein (CHOP) which controls genes related to the unfolded protein response[61]. For example, CHOP suppressed CEBPA, PPARα, and SREBF1, proteins involved in lipid metabolism[62], and upregulated the BH3-only pro-apoptotic proteins BIM, PUMA, and BAX[63]. ATF4 also induced transcription of genes implicated in autophagy such as *p62*, *Nbr1*, *Atg3*, *Atg7*, and *Becn1* for nutrient recycling[64] and genes involved in amino acid biosynthesis and transport such as *Asns* and *Gpt2*[65]. Overexpression of ATF4 strongly retarded

cell growth and elevated levels of reactive oxygen species[66]. The various cellular processes mediated by the AAR pathway such as amino acid and lipid metabolism, apoptosis, growth and proliferation, and autophagy may account for halofuginone's broad scope of biological activities.

GCN2 knockout mice remained sensitive to halofuginone and showed a block in Th17 differentiation that was comparable to wild-type mice (Whitman, unpublished data). Therefore, the canonical amino acid starvation response pathway that signals through GCN2 was unlikely to mediate Th17 differentiation. Since Th17 differentiation was rescued by proline addition, the responsible signaling intermediate must be downstream of EPRS and upstream of GCN2. GCN1, a highly expressed translational activator that transfers uncharged tRNAs from the ribosomal A site to GCN2, was a prime candidate[67]. GCN1 association with the ribosomal small protein RPS10 was also required for GCN2 activation[68]. NMR spectroscopy revealed that GCN1 binds to the RWD domain of GCN2[69]. The protein IMPACT also contains an RWD domain and competes against GCN2 for binding to GCN1. IMPACT is highly expressed in neurons and plays a role in neuritogenesis by weakening GCN2 activation, presumably through GCN1 scavenging[70]. Mass spectrometry data sets suggest that the large 296 kDa GCN1 protein containing more than 20 HEAT repeats may act as a scaffold with numerous binding partners[71]. Of immunological interest are interactions with PD-L1 (CD274)[72] and FoxP3[73]. FoxP3 is the master transcriptional regulator of the development and function of immunosuppressive regulatory T cells (Treg)[74] and PD-L1 is the ligand for the inhibitory PD1 receptor on cytotoxic $CD8^+$ T cells that dampens their effector functions[75]. Biochemical studies of mammalian GCN1 are required to validate these noteworthy interactions.

The majority of work on GCN1 has been conducted on its ortholog in yeast. Yeast Gcn1 forms a complex with Gcn20 that tethers yeast Gcn2 to the ribosome[76]. Truncation and

mutagenesis studies demonstrated that the C-terminus of Gcn1 binds to N-terminus Gcn2 and that the N-terminus of Gcn1 binds to the ribosome[77]. Association of Gcn1 with Gcn20 and polyribosomes is necessary for Gcn2 phosphorylation, full activation of eIF2α, and expression of Gcn4, the yeast ortholog of mammalian ATF4[78,79]. The adaptor protein Gir2 contains an RWD domain like Gcn2 and competes with Gcn2 for Gcn1 binding. Overexpression of Gir2 resulted in growth inhibition which was reversed by co-overexpression of Gcn2. Gir2 interacts with the ribosome-binding GTPase Rbg1 and co-fractionated with ribosomes in a Gcn1-dependent manner, suggesting that Gcn1/Gir2/Rbg1 together form a complex localized to ribosomes[80]. X-ray diffraction revealed Rbg1 coupled with Tma46, a regulatory protein that recruits Rbg1 to polyribosomes and increases GTP hydrolysis[81]. Amino acid starvation induced the association of Gir2 with another ribosome-binding GTPase Rbg2, and Gir2 binding to Rbg2 was significantly stronger than its binding to Rbg1. Mutation of the guanine nucleotide-binding domain of Rbg2 suggested that GDP/GTP stabilizes the Gir2/Rbg2 complex to promote efficient cell growth during amino acid starvation. The strength of the interaction between Gir2/Rbg2 and Gcn1 correlated with the concentration of 3-AT, a histidine depleting agent[82]. Signal transduction through Gir2 rather than Gcn2 has been termed the non-canonical amino acid starvation response pathway[83] (Figure I).

The mammalian orthologs in the non-canonical amino acid starvation response pathway are poorly characterized. Mammalian RWDD1, named after its RWD domain, is orthologous to yeast Gir2. The scant literature on RWDD1 describes it as a thymus aging related protein that is highly expressed in thymocytes and thymic epithelial cells, and it was weakly expressed in aged or oxidatively stressed mice[84]. Co-fractionation and yeast two-hybrid studies demonstrated that RWDD1 interacts with DRG1, the mammalian ortholog of yeast Rbg1[85,86]. Potassium strongly

enhanced the GTPase activity of DRG1 whereas mutation of a threonine phosphorylation site abrogated activity. LEROPO4, the mammalian ortholog of yeast Tma46, bound DRG1 at its C-terminal DFRP domain and increased the catalytic activity of DRG1 four-fold[87]. DRG1 expression was stabilized by LEROPO4 co-expression and the LEROPO4/DRG1 complex localized to polyribosomes[88].

Mass spectrometry databases suggest that RWDD1 also interacts with DRG2, the mammalian ortholog of Rbg2[89]. DRG2 deactivated the small GTPase Rab5 to stimulate recycling of transferrin, a blood plasma glycoprotein that maintains iron homeostasis[90]. DRG2 transgenic mice exhibited increased bone resorption by osteoclasts, resulting in significant bone loss. Osteoclasts in these animals showed greater survival and cytoskeletal reorganization in response to macrophage colony-stimulating factor[91]. In antigen presenting cells, DRG2 enhanced PPARα activity, diminished NF-κB activity, and reduced IL-6 production. DRG2 overexpression inhibited Th17 development and ameliorated experimental autoimmune encephalitis in mice[92], recapitulating the effects of halofuginone treatment. This last observation may hint that inhibition of Th17 differentiation by halofuginone may involve non-canonical AAR signaling through RWDD1 and DRG2.

Amino Acid Metabolism and Immunity

Halofuginone treatment simulates proline depletion, which correlates with amelioration of Th17-associated autoimmunity and attenuation of inflammation induced by TNF-α and IL-1β. Regulation of amino acid availability is beginning to surface as a general mechanism of immunomodulation. The most well-studied example is oxidative catabolism of tryptophan into *N*-formylkynurenine by the enzyme indoleamine 2,3-dioxygenase (IDO). Dendritic cells express

and release high levels of IDO in response to pro-inflammatory stimuli such as IFNγ, lipopolysaccharide (LPS), and TNF-α[93,94]. IDO-expressing dendritic cells drove the differentiation of naïve CD4+ helper T cells into FoxP3+ T regulatory cells (Treg), activated mature Treg and enhanced their suppressive functions, and blocked the reprogramming of Treg into non-suppressive T helper cells[95]. IDO reduced proliferation and IgM production of B cells activated by T independent antigens[96]. Tryptophan metabolites in the kynurenine pathway selectively induced apoptosis of Th1 but not Th2 cells in mice[97]. Tryptophan 2,3-dioxygenase (TDO) is another tryptophan-catabolizing enzyme expressed in the liver, brain, and skin[98,99]. Overexpression of TDO restricted T cell activation and inhibited growth of bacteria, parasites, and viruses[100]. Arginase-1 (ARG1) hydrolyzes arginine into ornithine and urea. Activated myeloid-derived suppressor cells upregulated ARG1 in the tumor microenvironment which decreased TCR expression and rendered tumor-specific effector T cells anergic[101]. Inducible nitric oxide synthase (iNOS) catalyzes the production of nitric oxide by catabolizing arginine. iNOS enhanced apoptosis of CD4 and CD8 memory T cells[102] and inhibited Th17 but not Th1 or Th2 differentiation[103]. Like proline depletion by halofuginone, tryptophan and arginine depletion by IDO and ARG1 respectively activated GCN2 signaling[104]. GCN2-knockout T cells cultured with IDO-expressing dendritic cells displayed resistance to anergy and continued to proliferate[105]. Borrelidin, a small molecule inhibitor of threonyl-tRNA synthetase, also suppressed Th17 differentiation. Addition of excess threonine rescued Th17 differentiation, recapitulating the effects of halofuginone and proline.[47,53] These findings highlight halofuginone's potential to serve as a convenient tool to study the amino acid starvation response pathway, a key regulator of immunity (Figure II).

Schematic Figures

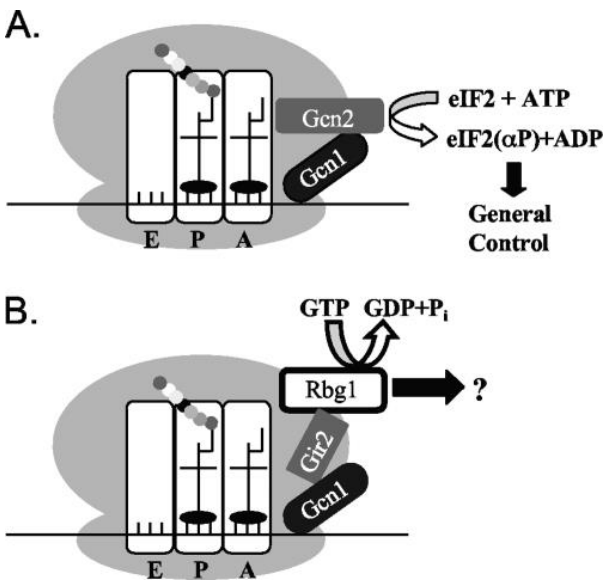

Figure I. Gcn1-dependent signaling during amino acid starvation in yeast. (**A**) In the canonical amino acid starvation response (AAR) pathway, Gcn1 interacts with Gcn2 on translating ribosomes to detect uncharged tRNAs. Gcn2 phosphorylates eIF2α which activates general control of amino acid metabolism. (**B**) In the non-canonical AAR pathway, Gir2 binds to Gcn1 and Rbg1. Rbg1 hydrolyzes GTP into GDP, but the downstream effects are unclear. *Figure adapted from Wout et al., 2009.*

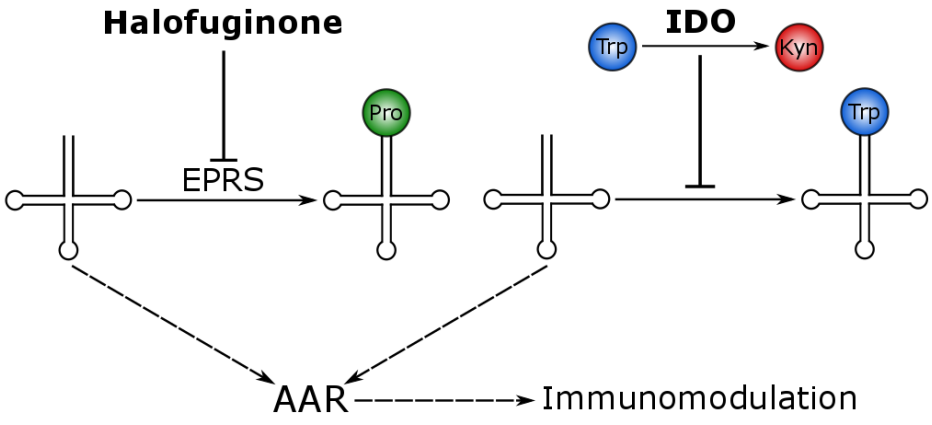

Figure II. Amino acid metabolism modulates immunity. Halofuginone treatment mimics proline starvation by inhibiting EPRS activity and IDO induces tryptophan starvation by catabolizing tryptophan into kynurenine. Both mechanisms lead to the accumulation of uncharged tRNAs, activating the amino acid starvation response (AAR) pathway which modulates the immune system.

Chapter Two: Data and Methods

Short Introduction

The overall goal of this study was to elucidate the signal transduction pathways evoked by halofuginone treatment that modulate the immune response. Since it was previously shown that halofuginone competed with proline for the catalytic site of glutamyl-prolyl-tRNA synthetase[53], we first tested the effects of halofuginone on *in vitro* proline translation. Because GCN2-dependent signaling could not account for all of halofuginone's immunomodulatory effects, we decided to focus on GCN1, a translational activator directly upstream of GCN2. We sought to demonstrate that GCN1 associated with ribosomes to sense uncharged tRNAs in the A site. Next, we wanted to validate halofuginone-induced signaling through the canonical amino acid starvation response (AAR) pathway by examining the physical interaction of GCN1 with GCN2 and the phosphorylation states of GCN2 and eIF2α. We then investigated the mammalian orthologs of the yeast non-canonical AAR pathway to check if complex formation was recapitulated. Abrogation of GCN1 expression and comparison to primary cells derived from GCN2 knockout mice would help dissociate GCN2-dependent from GCN2-independent phenotypes that rely on GCN1. We attempted to block signaling through GCN1 by overexpression of truncated binding partners, overexpression of full-length binding partners, and CRISPR-Cas9 knockout. We also tried to reduce expression of downstream proteins in the non-canonical AAR pathway by shRNA knockdown in fibroblast-like synoviocytes to model rheumatoid arthritis, and compared the response to inflammatory cytokines and halofuginone in knockdown versus control cells. Combined, these experiments should provide a framework to better understand the immunomodulatory role of GCN1-dependent signaling during halofuginone treatment.

Materials and Methods

Table 1. Cell Lines

Line	Description
K4	Immortalized human fibroblast-like synoviocytes
293T	Immortalized human embryonic 293 kidney cells containing SV40 large T-antigen

Table 2. Plasmids

ID #	Vector
13.16	pcDNA3-Flag-GCN2
17.53	pCSX-EGFP
18.42	pCSX-3V5-GCN2
18.43	pCSX-GCN2-3V5
20.20	pCSX-3Flag-GCN1
25.19	pHAGE-CMV-DRG2-Flag-HA-Puro
25.43	pCSX-GCN2(RWD)-3V5
25.44	pCSX-IMPACT(RWD)-3V5
25.45	pCSX-RWDD1(RWD)-3V5
25.46	pHAGE-CMV-GCN2(RWD)-3V5-SV50-Puro
25.47	pHAGE-CMV-IMPACT(RWD)-3V5-SV50-Puro
25.48	pHAGE-CMV-RWDD1(RWD)-3V5-SV50-Puro
26.18	pCSX-RWDD1-10His

Table 3. Antibodies

Epitope	Species	Dilution	Manufacturer
Flag	mouse	1:5000	Sigma-Aldrich
V5	rabbit	1:5000	Thermo Fischer Scientific
His	rabbit	1:2000	Covance
GCN1	rabbit	1:5000	Novus Biologicals
GCN2	rabbit	1:1000	Cell Signaling Technology
pGCN2	rabbit	1:1000	Epitomics
eIF2α	rabbit	1:1000	Cell Signaling Technology
p-eIF2α	rabbit	1:1000	Cell Signaling Technology
EPRS	rabbit	1:5000	Sigma-Aldrich
L13a	rabbit	1:5000	Cell Signaling Technology
RWDD1	rabbit	1:1000	Cell Signaling Technology
DRG2	rabbit	1:1000	GeneTex
calreticulin	rabbit	1:1000	Cell Signaling Technology
β-actin	mouse	1:10000	Abcam
GAPDH	mouse	1:5000	GeneTex

Table 4. Oligonucleotides

Target	ID #	Sequence
GCN1	gRNA-1	5′-CACCGACCATCCACGGCGTGCTTGT-3′ 3′-CTGGTAGGTGCCGCACGAACACAAA-5′
GCN1	gRNA-2	5′-CACCGCTGGTGTAACCGATTCACTA-3′ 3′-CGACCACATTGGCTAAGTGATCAAA-5′
-	shRNA-scr	5′-CCTAAGGTTAAGTCGCCCTCG-3′
RWDD1	shRNA-682	5′-ACTGTATGTAAACTTGAGGGT-3′
RWDD1	shRNA-683	5′-CACTGTATGTAAACTTGAGGG-3′
RWDD1	shRNA-684	5′-TGTATGTAAACTTGAGGGTAG-3′
RWDD1	shRNA-685	5′-TAATGGTGAAGCTGGGTGGAT-3′
RWDD1	shRNA-686	5′-CTCAGACGTCACAGTAATGGT-3′
CXCL10	primer-61/62	F: 5′-GAAAGCAGTTAGCAAGGAAAGGT-3′ R: 5′-GACATATACTCCATGTAGGGAAG-3′
MMP-13	primer-67/68	F: 5′-CCAGTCTCCGAGGAGAAACA-3′ R: 5′-AAAAACAGCTCCGCATCAAC-3′
GAPDH	primer-19/20	F: 5′-AGCCACATCGCTCAGACAC-3′ R: 5′-GCCCAATACGACCAAATCC-3′

Cell Culture. K4 and 293T cells were grown at 37°C / 5% CO_2 and maintained in Dulbecco's Modified Eagle Medium (DMEM) (Lonza) supplemented with 10% fetal bovine serum (Gibco), 2 mM L-glutamine (Lonza), and 1% penicillin/streptomycin (Thermo Scientific).

Sub-cloning. Destination vectors were digested with appropriate restriction enzymes at 37°C for 2 hours. Linearized vectors were dephosphorylated with Antarctic phosphatase (New England BioLabs) at 37°C for 30 minutes and gel purified with the QIAquick kit (Qiagen). Inserts were phosphorylated with T4 PNK (New England BioLabs) at 37°C overnight. Ligation was performed with T4 DNA ligase (New England Biolabs) at 14°C overnight. DH5α were

transformed with recombinant vectors and mini-prepped with the QIAprep kit (Qiagen). Inserts were confirmed by restriction fragment length analysis and DNA sequencing.

Western Blot. Cells extracts were prepared with 1x PhosStop (Roche), 1x Complete EDTA-free protease inhibitor cocktail (Roche), 1 mM PMSF, and 1 mM NEM. Samples were mixed with Laemmli buffer, denatured at 70°C for 5 minutes, run on 4-12% or 12% SDS-PAGE gels, and transferred to nitrocellulose membrane. Membranes were blocked with 5% milk–Tris-buffered saline supplemented with 0.1% Tween (TBS-T) for 1 hour at room temperature and incubated overnight with primary antibodies (Table 3). Primary antibodies were washed with TBS-T, and membranes were incubated with 1:5000 anti-rabbit or anti-mouse IgG conjugated to horseradish peroxidase (Cell Signaling Technologies) for 1 hour at room temperature. All antibodies were diluted in TBS-T supplemented with 2% BSA and 5 mM EDTA. Signal was detected and captured digitally with the PXi imaging system (SynGene).

***In vitro* Translation.** Proline-containing (Pro) and proline-deficient (NoPro) gBlock Gene Fragments (Integrated DNA Technologies) were sub-cloned into the pT7CFE1-CHis plasmid (Thermo Fischer Scientific) by EcoRV (New England BioLabs) digestion. Reaction mixes were prepared using the 1-Step Human Coupled IVT kit (Thermo Fischer Scientific). 5 μM halofuginone and 5 mM L-proline were added. Samples were incubated at 30°C for 90 minutes and digested with 90 U/ml benzonase nuclease (Novagen) at 4°C for 1 hour. Samples were diluted 1:5 in RIPA buffer (Roche) and run on 12% SDS-PAGE gel for western blot.

Viral Transduction. 10 cm dishes were coated with 10 μg/ml poly-D-lysine before seeding 293T cells to 70% confluency. For gene overexpression, transfection was performed with 40 μl Lipofectamine 2000 (Thermo Fischer Scientific) and 4 μg pHAGE-gene, 5 μg pHDM-Hgpm2 (CMV-HIV gag/pol), 5 μg pCMV-tat, 5 μg pCMV-rev, and 5 μg pCMV-VSGg. For gene knockdown, transfection was performed with 60 μl Effectene (Qiagen) and 888 ng pLKO.1-gene, 444 ng pMD2.G, and 666 ng psPAX2. Viral supernatant was harvested 48 hours post-transfection and filtered with a 0.45 μM syringe filter. Polybrene was added to a final concentration of 5 μg/ml. K4 cells plated at 70% confluency were transduced for 6 hours. 24 hours post-transduction, K4 cells were selected with 2 μg/ml puromycin for at least 72 hours.

Co-Immunoprecipitation. K4 cells seeded to 70% confluency in 6-well plates were transfected with 2 ul Lipofectamine 2000 (Thermo Fischer Scientific) and 4 ug plasmid DNA for 24 hours. pCSX-GFP was used to normalize DNA amounts and check for transfection efficiency. Cells were treated with 200 nM halofuginone for 1 hour. Protein extracts were harvested with IP lysis buffer (25 mM Tris-HCl pH 7.4, 150 mM NaCl, 1 mM EDTA, 1% NP-40, 5% glycerol) and protease and phosphatase inhibitors as described above. Extracts were pre-cleared with non-specific Protein-A Sepharose beads (Rockland) and transferred to anti-Flag beads (Clontech) blocked with 2% BSA for over-night immunoprecipitation. Beads were washed with IP lysis buffer and eluted with 1% SDS. Elution was run on 4-12% SDS-PAGE gel for western blot.

Column Extraction. K4 cells were permeabilized with digitonin buffer (110 mM KOAc, 25 mM KHEPES pH 7.2, 2.5 mM $Mg(OAc)_2$, 1 mM EGTA, 0.015% digitonin, 1 mM DTT, 1mM PMSF). Poly-Prep chromatography columns (Bio-Rad) were loaded with Sepharose CL-6B (Sigma-Aldrich) and calibrated with dextran blue and Ponceau S. Cell extracts were passed

through the column by gravity and 2-drop fractions were collected. Fractions were run on 4-12% SDS-PAGE gel for western blot.

Sequential Extraction. K4 cells were sequentially permeabilized with digitonin buffer (110 mM KOAc, 25 mM KHEPES pH 7.2, 2.5 mM $Mg(OAc)_2$, 1 mM EGTA, 0.015% digitonin, 1 mM DTT, 1mM PMSF, 40 U/ml RNAse inhibitor) for 5 minutes, washed with wash buffer (110 mM KOAc, 25 mM KHEPES pH 7.2, 2.5 mM $Mg(OAc)_2$, 1 mM EGTA, 0.004% digitonin, 1 mM DTT, 1 mM PMSF) for 1 minute, and lysed with NP-40 buffer (400 mM KOAc, 25 mM KHEPES pH 7.2, 15 mM $Mg(OAc)_2$, 1% NP-40, 0.5% DOC, 1 mM DTT, 1 mM PMSF, 40 U/ml RNAse inhibitor) for 5 minutes. Extracts collected after the permeabilization and lysis stages were run on 4-12% SDS-PAGE gel for western blot.

CRISPR-Cas9 Knockout. Guide RNAs were sub-cloned into the pX330 vector (Addgene). K4 cells were co-transfected with pX330 and pNTAP-GFP using Effectene (Qiagen). 36 hours post-transfection, cells were selected with 2 μg/ml puromycin for 48 hours. Cells were diluted to 1 cell per well of a 96-well plate and clonally expanded to 6-well plates. Cells were lysed with RIPA buffer (Roche) and protease and phosphatase inhibitors as described above. Extracts were run on 4-12% SDS-PAGE gel for western blot.

Quantitative Polymerase Chain Reaction. RNA was extracted from K4 cells using TRIzol (Life Technologies) and the Direct-zol RNA mini-prep kit (Zymo Research). RNA was converted to cDNA by RT-PCR. cDNA was amplified by qPCR with fluorescent reporter probes. CT values were calculated and normalized to GAPDH for analysis.

Results

Effect of Halofuginone on Proline Utilization for Translation

Halofuginone bound the catalytic site of the prolyl-tRNA synthetase domain (ProRS) of EPRS[53]. We hypothesized that halofuginone would inhibit EPRS function and prevent charging of prolyl-tRNA, abrogating the translation of mRNA containing proline codons. To investigate this proposed mechanism, we designed two gene blocks using a portion of the albumin amino acid sequence as a backbone; one contained two pairs of proline residues (Pro) and the other lacked proline completely (NoPro) (Figure 1A). The gene blocks were tagged with N-terminal Flag epitopes, sub-cloned into the pT7CFE vector with a 5' UTR internal ribosome entry site (IRES), and expressed in a cell-free *in vitro* translation system. Translation was assessed by anti-Flag western blot. Without halofuginone treatment, both gene blocks were translated into peptides at the expected size of ~25 kDa. Halofuginone treatment specifically blocked complete translation of the Pro gene block but not the NoPro gene block (Figure 1B). A weakly expressed truncation product at ~20 kDa corresponded to termination of translation at the site of the C-terminal proline residues. The strong reduction in band intensity may be attributed to decay of nascent peptides at stalled ribosomes. These results suggested that halofuginone selectively prevented incorporation of proline into elongating peptides during translation.

Unexpectedly, an additional band appeared when halofuginone blocked translation of the Pro gene block. The upper band shift of ~25 kDa above the expected truncation size roughly correlated to the size of a tRNA. We presumed that when uncharged prolyl-tRNA entered the A site of the ribosome, no peptide bond could be formed with the growing peptide for translocation from the P site to the A site. In this case, the previous tRNA would still be linked to the peptide in the P site, and this tRNA-peptide complex may dissociate from the ribosome or be degraded.

To test the former possibility, we added benzonase nuclease to the reaction mix after *in vitro* translation. We observed a strong reduction of the upper band with a reciprocal enrichment in the lower band (Figure 1C). An intermediate band also appeared, likely resulting from incomplete digestion of the tRNA secondary structure. Therefore, halofuginone treatment may generate tRNA-peptide complexes as a byproduct of halted proline translation.

Since halofuginone competed with proline for binding to purified ProRS, we postulated that addition of excess proline would reverse the effects of halofuginone on translation of the Pro gene block. Indeed, proline at 1000-fold greater concentration than halofuginone rescued translation of the Pro gene block (Figure 1D). Taken together, these findings support a mechanism in which halofuginone prevents utilization of proline by EPRS, prohibiting the charging of prolyl-tRNA and the translation of proline codons.

Subcellular Localization of Ribosomes and GCN1-Signaling Components

Halofuginone had a profound effect on translation, so we next examined the ribosome to decipher the drug's molecular mechanism. To isolate ribosomes, we extracted the cytoplasm of K4 human fibroblast-like synoviocytes using a permeabilization buffer containing digitonin. Cytoplasmic extracts were passed through a column packed with Sepharose beads; larger components such as ribosomes eluted faster than smaller components such as free proteins. The absorbance at 280 nm (A280) of fractions was measured to pinpoint eluted proteins to predominantly fractions 3-12. L13a, a marker for the 60S large ribosomal subunit, appeared early in fractions 3-4. GCN1, GCN2, and EPRS also appeared in fractions 3-4, implying their association with the ribosome (Figure 2A). Free GCN1, GCN2, and EPRS was also detected in

later fractions. As expected, small housekeeping genes such as β-actin and GAPDH did not co-fractionate with ribosomes, mostly appearing in fractions 7-10.

We also tracked ribosomes and GCN1-signaling components using sequential extraction. The cytosolic fraction of K4 cells was extracted with digitonin buffer and the endoplasmic reticulum (ER) fraction was subsequently extracted with NP-40 buffer. Cytosolic fractions exclusively contained β-actin and ER fractions exclusively contained calreticulin (also known as endoplasmic reticulum resident protein 60). L13a appeared in both fractions, suggesting that cytosolic ribosomes and ER-bound ribosomes were differentially extracted. GCN1 and EPRS were also found in both fractions, consistent with their role in translation. During halofuginone treatment, there was a shift of L13a from the ER fraction to the cytosolic fraction (Figure 2B). Interestingly, GCN1 recapitulated this trend, lending further support that GCN1 binds to ribosomes. Surprisingly, other GCN1 signaling components that participate in canonical and non-canonical AAR such as GCN2, RWDD1, and DRG2 appeared solely in the cytosolic fraction. The column fractionation and sequential extraction studies support a mechanism in which uncharged tRNAs generated by halofuginone activate AAR pathways through GCN1 poised on cytoplasmic ribosomes.

GCN1 and the Canonical Amino Acid Starvation Response

In yeast, Gcn1 tethers Gcn2 to the ribosome, and Gcn1 was necessary for Gcn2 activation in the canonical AAR pathway[76]. We evaluated GCN1 binding to GCN2 in mammalian cells by co-immunoprecipitation. K4 cells were co-transfected to overexpress human GCN1 tagged with a 3xFLAG epitope (Flag-GCN1) and GCN2 tagged with a 3xV5 epitope (V5-GCN2). As a negative control, cells were transfected with V5-GCN2 only. Cell lysates were

immunoprecipitated with anti-Flag beads, and V5-GCN2 co-immunoprecipitated with Flag-GCN1 (Figure 3A). Binding was specific because V5-GCN2 was not detected after immunoprecipitation when Flag-GCN1 was not co-transfected. These findings illustrated that overexpressed GCN1 associated with overexpressed GCN2, recapitulating the interaction between yeast Gcn1 and Gcn2. Halofuginone did not appear to significantly influence this association.

Yeast Gcn2 dimerizes with itself through paired interactions of the protein kinase domain with the ribosome-binding domain[106]. Dimerization of Gcn2 is essential for tRNA binding and kinase activity[107]. To test if GCN2 also dimerizes in mammals, K4 cells were co-transfected to overexpress human GCN2 tagged with a 3xFLAG epitope (Flag-GCN2) and V5-GCN2. As a positive control, cells were co-transfected with Flag-GCN1 and V5-GCN2. As a negative control, cells were transfected with V5-GCN2 only. Cell lysates were immunoprecipitated with anti-Flag beads, and V5-GCN2 co-immunoprecipitated with Flag-GCN2 (Figure 3B). Binding was specific because V5-GCN2 was not detected after immunoprecipitation if Flag-GCN2 was not co-transfected. As expected, V5-GCN2 also co-immunoprecipitated with Flag-GCN1, although this interaction appeared weaker than that of V5-GCN2 and Flag-GCN2. Addition of halofuginone appeared to promote formation of V5-GCN2/Flag-GCN2 dimers (Figure 3C). These data suggest that GCN2 dimerizes in mammals as observed in yeast, and halofuginone may induce dimerization to increase GCN2's affinity for tRNA and kinase activity to stimulate the canonical AAR pathway.

During amino acid starvation in yeast, Gcn1 triggers the phosphorylation of Gcn2, and activated Gcn2 then phosphorylates eIF2α to upregulate genes that control amino acid metabolism[59]. We mimicked proline starvation in K4 cells with treatment of 200 nM

halofuginone for 1 hour. Halofuginone strongly induced phosphorylation of GCN2 and phosphorylation of eIF2α. These findings indicate that halofuginone activates the canonical AAR pathway through GCN2 in mammalian cells.

GCN1 and the Non-Canonical Amino Acid Starvation Response

In yeast, the adaptor protein Gir2 bridges Gcn1 and the GTPase Rbg2 to transmit non-canonical AAR signals at the ribosome[80]. We investigated formation of this ternary complex in mammalian cells with a series of co-immunoprecipitation studies. K4 cells were co-transfected to overexpress Flag-GCN1 and RWDD1 tagged with a 10xHis epitope (His-RWDD1). RWDD1 is the mammalian ortholog of yeast Gir2. As a negative control, cells were transfected with His-RWDD1 only. Cell lysates were immunoprecipitated with anti-Flag beads, and His-RWDD1 co-immunoprecipitated with Flag-GCN1 (Figure 4A). Binding was specific because His-RWDD1 did not immunoprecipitate if Flag-GCN1 was not co-transfected. These results suggested that overexpressed GCN1 interacted with overexpressed RWDD1. Halofuginone did not appear to significantly modulate this association.

We next probed the GCN1/RWDD1 complex for DRG2, the mammalian ortholog of Rbg2. DRG2 tagged with a FLAG epitope (Flag-DRG2) and His-RWDD1 were overexpressed in K4 cells by co-transfection. In parallel, cells were transfected with only His-RWDD1 as a negative control. Cell lysates were immunoprecipitated with anti-Flag beads, and His-RWDD1 co-immunoprecipitated with Flag-DRG2 (Figure 4B). Binding was specific because His-RWDD1 was undetectable after immunoprecipitation if Flag-DRG2 was not co-transfected. Endogenous GCN1 also co-immunoprecipitated with Flag-DRG2, and halofuginone did not appear to significantly alter these interactions. Taken together, these co-immunoprecipitation

studies demonstrate that in mammalian cells, overexpressed GCN1, RWDD1, and DRG2 form a complex that is orthologous to the yeast Gcn1/Gir2/Rbg2 complex involved in the non-canonical AAR pathway.

Approaches to Blocking GCN1-Dependent Signaling

Since GCN1 is at the intersection of the canonical and non-canonical AAR pathways, we sought to block signaling through GCN1 to reveal what phenotypes are linked to amino acid starvation induced by halofuginone. GCN1 is proposed to associate with the RWD domains of GCN2, IMPACT, and RWDD1[69,70,84]. In our first approach, we created gene blocks containing the RWD domains of GCN2, IMPACT, and RWDD1 tagged with 3xV5 epitopes (GCN2-RWD, IMPACT-RWD, and RWDD1-RWD) (Figure 5A) and sub-cloned them into the pHAGE vector for lentiviral transduction of K4 cells. Stable expression at the expected truncation sizes was confirmed by anti-V5 western blot. EGFP was also transduced as a negative control and produced no V5 signal. The GCN2-RWD and IMPACT-RWD were strongly expressed whereas RWDD1-RWD expression was relatively weak (Figure 5B). We proceeded with GCN2-RWD and IMPACT-RWD and tested their ability to attenuate canonical AAR signaling in response to three doses of halofuginone (50 nM, 100 nM, and 200 nM) for 1 hour. Unfortunately, overexpression of GCN2-RWD and IMPACT-RWD were unable to abrogate GCN1 signaling, as shown by the dose-dependent increase of GCN2 phosphorylation that was comparable to controls (Figure 5C). We presumed that the RWD domains of GCN2 and IMPACT were not sufficient for stable binding to GCN1.

In our second approach, we overexpressed full-length IMPACT and RWDD1 in an attempt to prevent GCN2-dependent signaling. IMPACT tagged with a 3xV5 epitope (V5-

IMPACT) or His-RWDD1 were overexpressed in K4 cells by co-transfection with a puromycin resistance plasmid to select for transfectants. EGFP was also transfected as a negative control. Overexpression was verified by anti-V5 and anti-His western blot. We treated transfectants with 100 nM of halofuginone for 1 hour and assessed canonical AAR signaling. Unfortunately, overexpression of full-length IMPACT and RWDD1 did not reduce phosphorylation of GCN2 relative to controls (Figure 5D). We attributed this outcome to potentially low co-transfection frequency; perhaps a considerable proportion of cells survived negative selection but did not receive the IMPACT and RWDD1 overexpression plasmids, leading to insufficient scavenging of endogenous GCN1.

We next attempted to knock out GCN1 with CRISPR-Cas9 genome editing and designed one guide RNA that targeted exon 6 of GCN1 (gRNA-1) and another targeting exon 14 (gRNA-2). The guide RNAs were sub-cloned into the pX330 Cas9 plasmid for co-transfection of K4 cells alongside a puromycin resistance plasmid. After puromycin selection, single cell clones were expanded and screened for GCN1 expression by western blot. For both guide RNAs, clones exhibited varying levels of GCN1, but no clone exhibited a complete loss of expression (Figure 5E). We observed a positive correlation between the level of GCN1 expression and the rate of cell growth. Clones 5, 8, and 9 for gRNA-1 and clone 1 for gRNA-2 were selected for further study, but all failed to continue surviving in culture. Because GCN1 is a highly expressed scaffold protein that also functions as a translational activator[71], we speculate that GCN1 knockout is lethal to cells. Consistent with our findings, GCN1 was found to be necessary for the proliferation of two cell lines in a large-scale CRISPR-based screen of essential genes in the human genome[108].

Blocking the Non-Canonical Amino Acid Starvation Response

Since we were unable to sufficiently inhibit GCN1 function, we shifted our focus to the downstream molecule RWDD1 in the non-canonical AAR pathway. Five small hairpin RNAs (shRNA 682, 683, 684, 685, and 686) targeting the *Rwdd1* transcript and a control scrambled shRNA were inserted into the pLKO.1 vector for RNA interference. The shRNA sequences were stably expressed in K4 cells by lentiviral transduction. Expression of RWDD1 was analyzed by western blot and normalized to expression of β-actin and GAPDH. Three shRNAs (682, 683, and 684) caused knockdown of RWDD1 relative to scrambled shRNA (Figure 6A).

The RWDD1 knockdown cell line generated by shRNA 683 (sh683) and the scrambled control cell line were treated with 100 nM or 200 nM halofuginone for 24 hours. After 16 hours of halofuginone treatment, cells were stimulated by 10 ng/μl TNF-α for 8 hours. Expression of the pro-inflammatory cytokine *CXCL10* and matrix metalloproteinase *MMP-13*, genes implicated in rheumatoid arthritis, was measured by qPCR. In both controls and sh683, *CXCL10* and *MMP-13* expression was strongly induced by TNF-α. Relative to the untreated baselines, sh683 showed weaker induction of *CXCL10* and *MMP-13* than controls. Notably, treatment with 200 nM halofuginone reduced *CXCL10* expression by 10.6-fold in controls but by only 1.3-fold in sh683 (Figure 6B). Likewise, halofuginone decreased *MMP-13* expression by 8.2-fold in controls but only 2.9-fold in sh683 (Figure 6C). These preliminary results suggest that RWDD1 may participate in a signaling pathway responsible for the immunomodulatory effects of halofuginone.

Brief Discussion

Our findings in this study expanded the possible molecular mechanisms of halofuginone (Figure 7). First, we further validated that halofuginone inhibits the activity of the prolyl-tRNA synthetase domain of EPRS. Halofuginone prevented complete translation of gene blocks containing proline but had no effect on gene blocks lacking proline. Rescue of translation with excess proline suggested that halofuginone is a competitive inhibitor of the prolyl-tRNA synthetase active site. Because proline addition also ameliorated the halofuginone-induced block in Th17 differentiation[53], we believe that the majority of physiological effects of halofuginone arise from the downstream consequences of uncharged prolyl-tRNA accumulation.

Uncharged tRNA may activate the translational activator GCN1, a protein with many binding partners that could account for the many effects of halofuginone. Supporting its suitability as a key mediator, column fractionation and differential extraction experiments implied the association of GCN1 with ribosomes. Furthermore, halofuginone stimulated phosphorylation of GCN2 and eIF2α, proteins downstream of GCN1 involved in proline biosynthesis[109]. The yeast literature provided a map of potential pathways that GCN1 may modulate in mammals. We confirmed that the protein interactions in yeast are preserved in mammalians using co-immunoprecipitation. In the canonical AAR pathway, mammalian GCN1 associated with GCN2, recapitulating yeast Gcn1 and Gcn2. In the non-canonical AAR pathway, mammalian GCN1 associated with RWDD1 and DRG2, imitating the yeast Gcn1/Gir2/Rbg2 complex. Since knockdown of RWDD1 may diminish the effects of halofuginone, the non-canonical AAR pathway may serve as a novel avenue of immunomodulation.

Figures

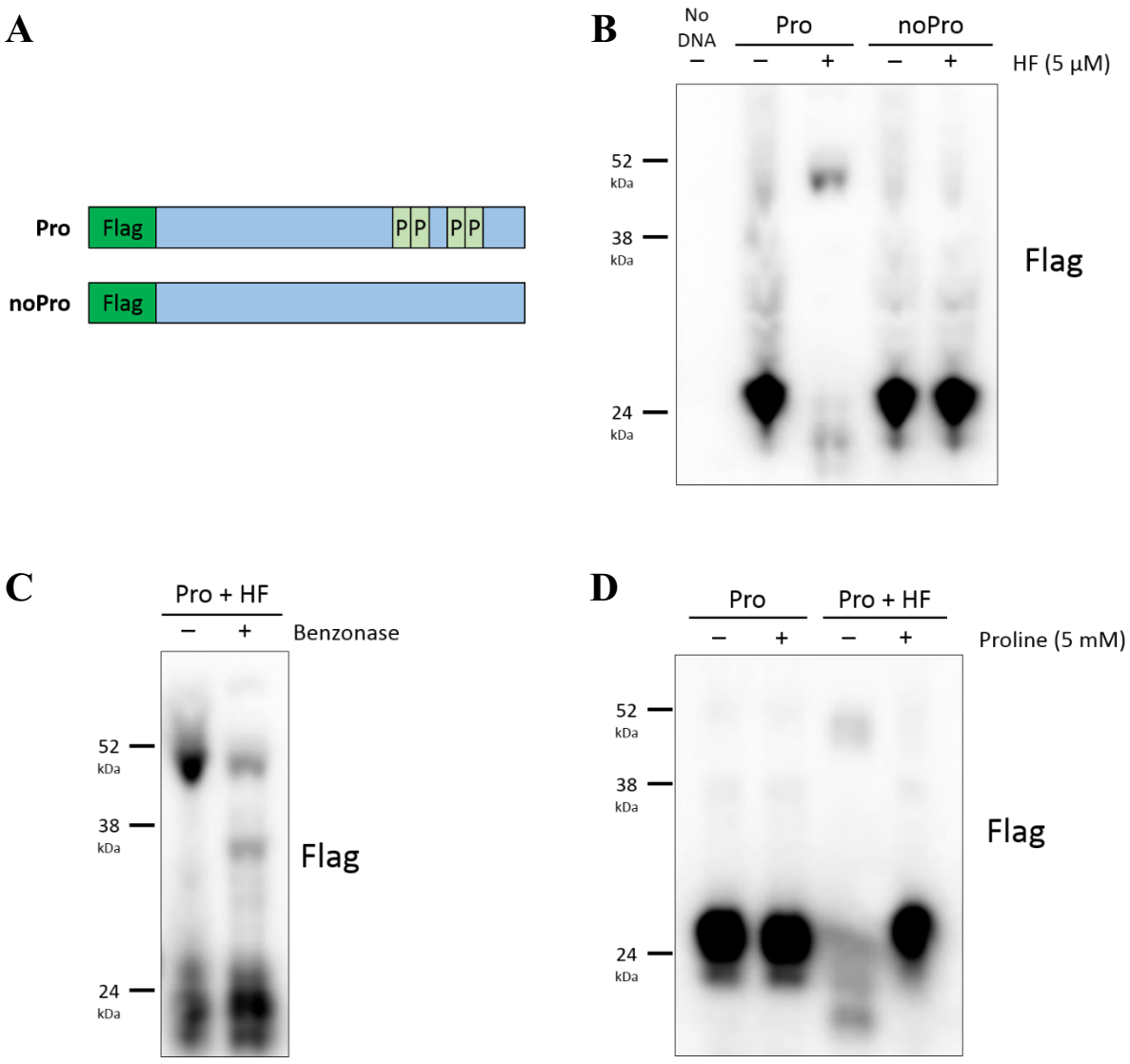

Figure 1. Effect of halofuginone on proline utilization for translation. (**A**) Flag-tagged gene blocks were designed for cell-free *in vitro* translation. One gene block contained two pairs of proline residues (Pro) and the other lacked proline completely (NoPro). (**B**) 5 µM halofuginone (HF) was added to the *in vitro* translation reactions. Products were analyzed by anti-Flag western blot. (**C**) After *in vitro* translation, reaction mixtures were digested with benzonase nuclease. (**D**) *In vitro* translation reactions with or without 5 µM halofuginone were supplemented with 5 mM *L*-proline.

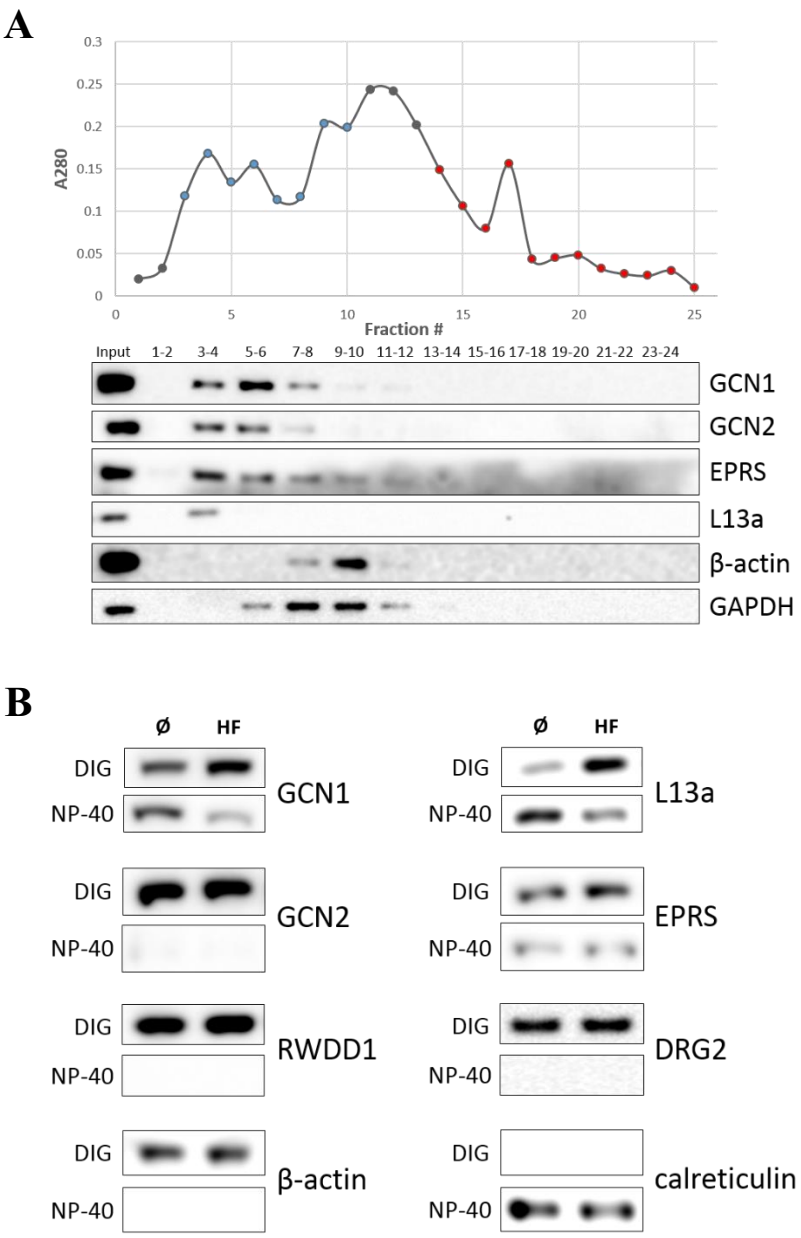

Figure 2. Subcellular localization of ribosomes and GCN1-signaling components. (**A**) Cytoplasmic extract of K4 cells was run through a Sepharose 6B column and 24 fractions were collected. The absorbance at 280 nm (A280) was measured for all fractions. The column was calibrated with dextran blue (blue points) and Ponceau S (red points). Fractions were screened for eluted proteins by western blot. L13a: large 60S subunit ribosomal marker. (**B**) K4 cells were treated with 200 nM halofuginone (HF) for 1 hour or untreated (Ø). The cytoplasmic fraction was extracted by digitonin permeabilization buffer (DIG). The endoplasmic reticulum (ER) fraction was sequentially extracted by NP-40 lysis buffer (NP-40). Protein localization was compared by western blot. β-actin: cytoplasmic marker. Calreticulin: ER marker.

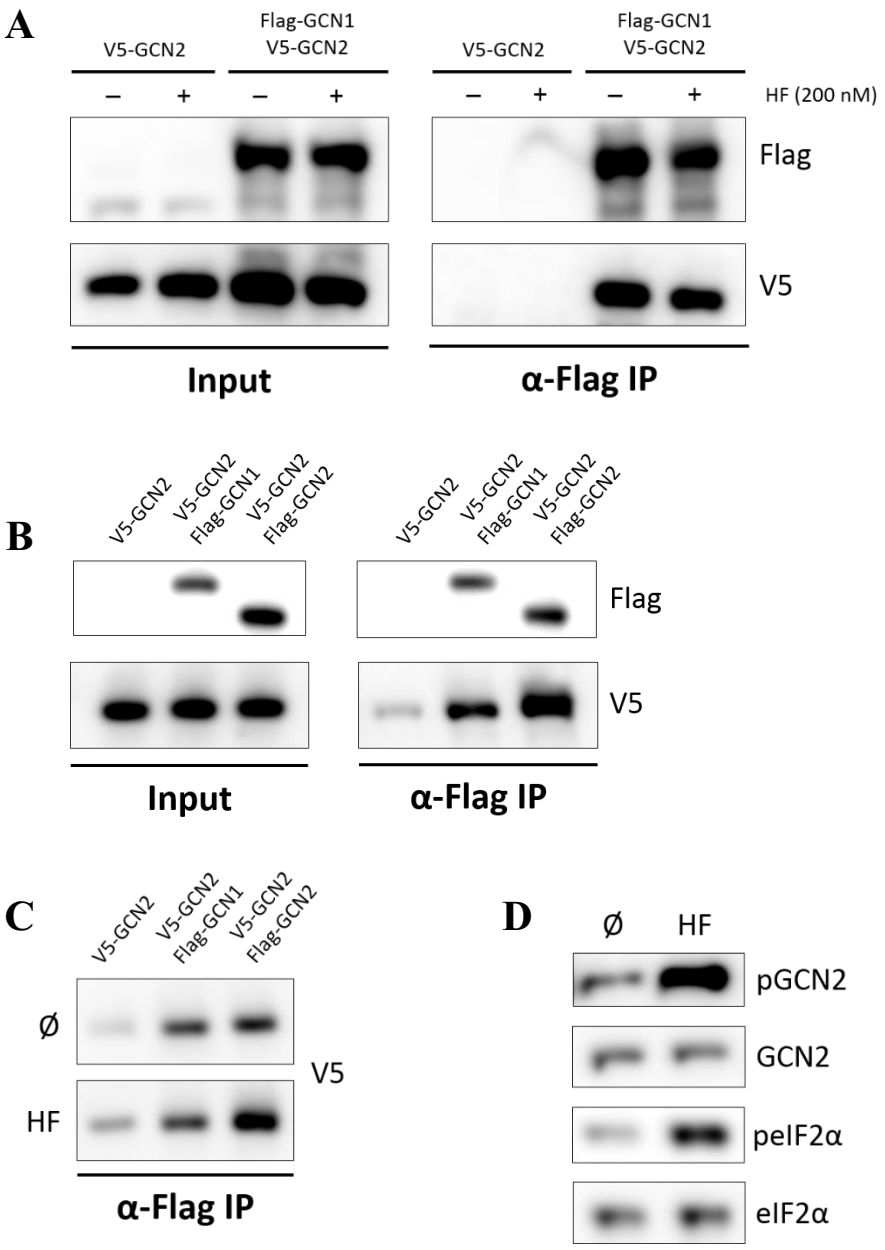

Figure 3. GCN1 and the canonical amino acid starvation response. (**A**) K4 cells were transfected with V5-GCN2 and Flag-GCN1 and were treated with 200 nM halofuginone (HF) for 1 hour. Protein extracts were immunoprecipitated with anti-Flag beads and analyzed by anti-Flag and anti-V5 western blot. (**B-C**) K4 cells were transfected with V5-GCN2, Flag-GCN1, and Flag-GCN2 and were treated with halofuginone or untreated (Ø) as in **A**. Immunoprecipitation and western blot as in **A**. (**D**) Phosphorylation of GCN2 and eIF2α after halofuginone treatment as in **a** was assessed by western blot.

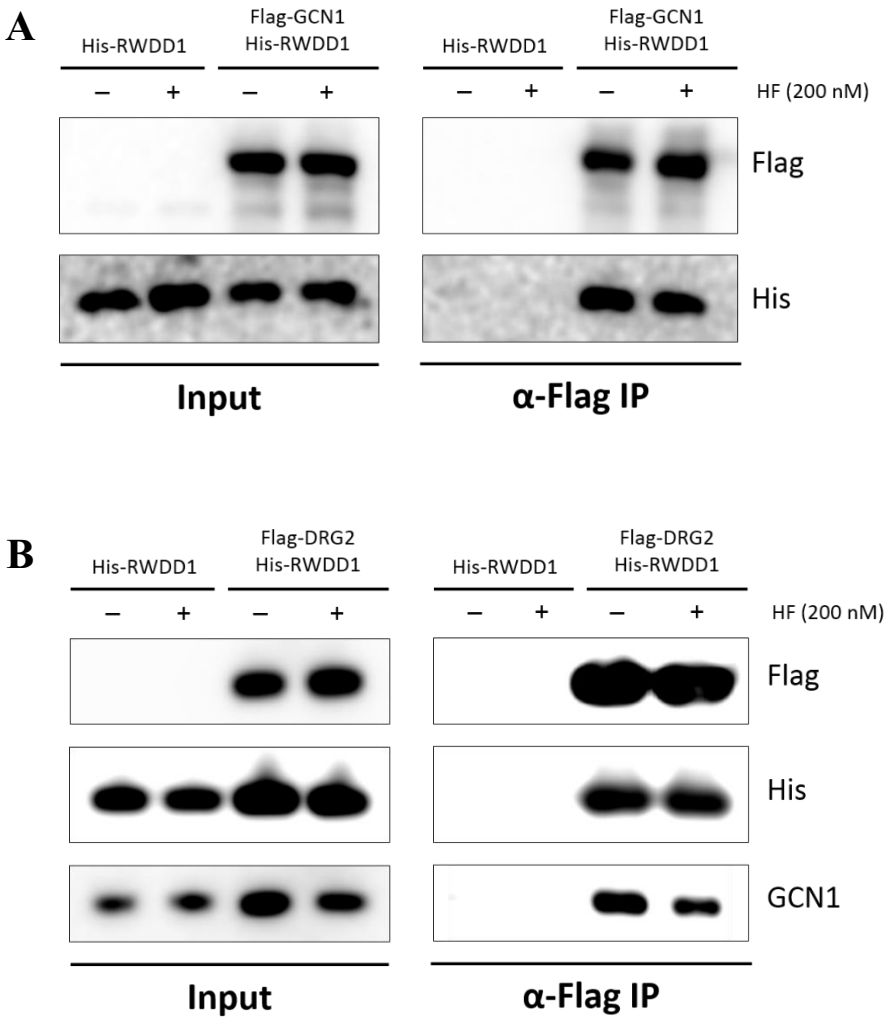

Figure 4. GCN1 and the non-canonical amino acid starvation response. (**A**) K4 cells were transfected with His-RWDD1 and Flag-GCN1 and were treated with 200 nM halofuginone (HF) for 1 hour. Protein extracts were immunoprecipitated with anti-Flag beads and analyzed by anti-His and anti-Flag western blot. (**B**) K4 cells were transfected with His-RWDD1 and Flag-DRG2 and were treated with halofuginone as in **A**. Immunoprecipitation and western blot as in **A**. Endogenous GCN1 was detected by anti-GCN1 western blot.

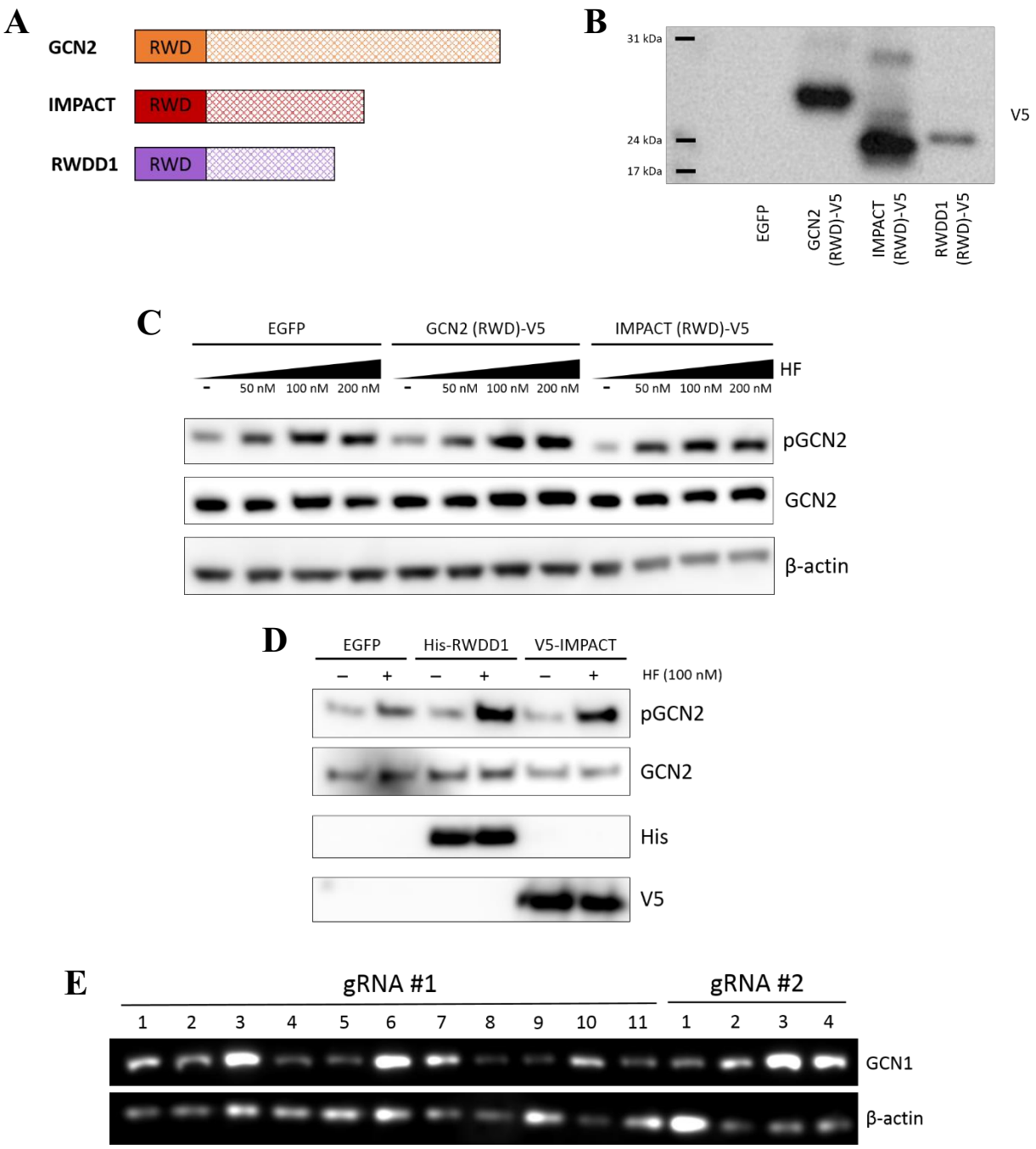

Figure 5. Approaches to blocking GCN1-dependent signaling. (**A**) GCN2, IMPACT, and RWDD1 were truncated to only their RWD domains. (**B**) K4 cells were transduced with V5-tagged RWD domains or EGFP. Stable expression of RWD domains was determined by anti-V5 western blot. (**C**) K4 cells were transfected with EGFP or RWD domains. Phosphorylation of GCN2 in response to incremental doses of halofuginone (HF) for 1 hour was assessed by western blot. (**D**) K4 cells were transfected with EGFP, full-length His-RWDD1, or full-length IMPACT. Phosphorylation of GCN2 in response to 100 nM halofuginone for 1 hour was assessed by western blot. (**E**) K4 cells were transfected with two guide RNAs (gRNAs) targeting GCN1 for CRISPR-Cas9 gene knockout. GCN1 expression was compared to β-actin expression by western blot.

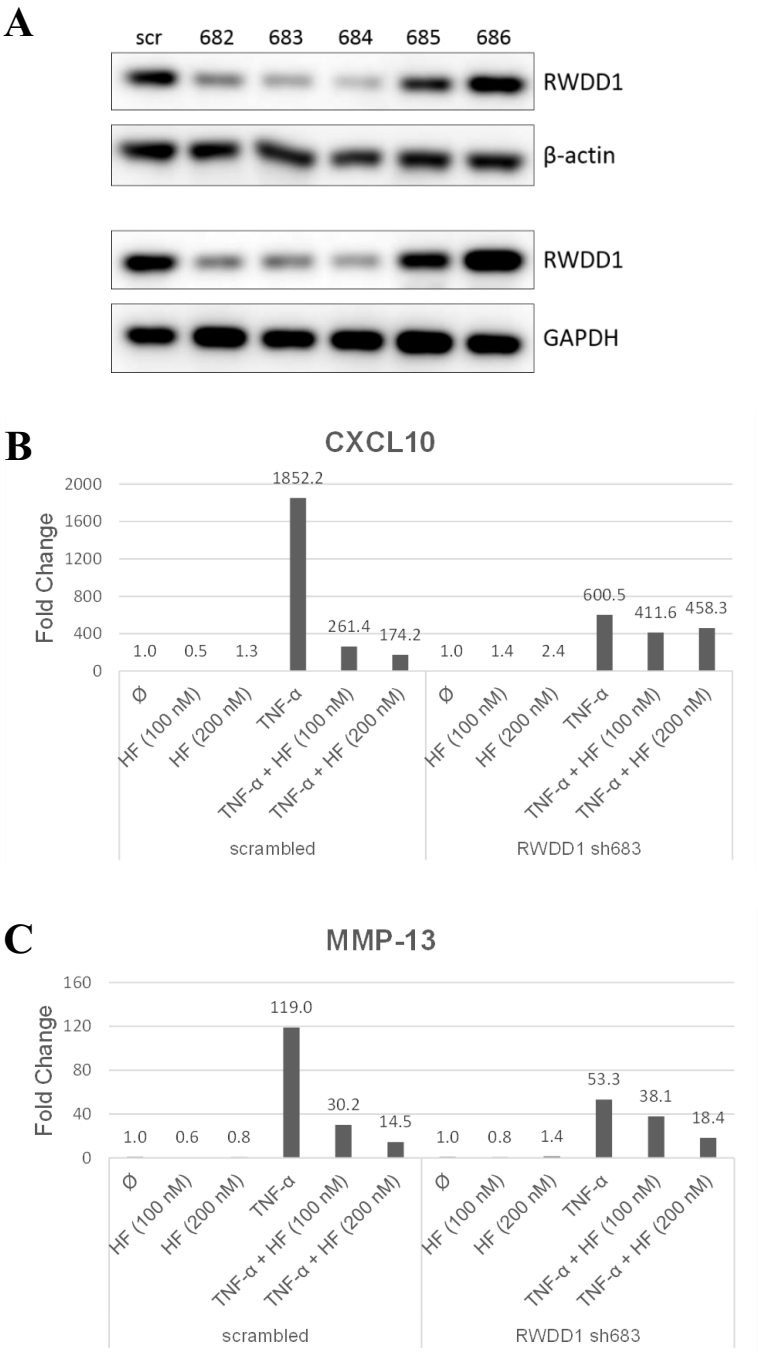

Figure 6. Blocking the non-canonical amino acid starvation response. (**A**) K4 cells were transduced with five shRNAs targeting the *Rwdd1* transcript (682, 683, 684, 685, and 686) or a scrambled (scr) shRNA as a control. RWDD1 expression was compared to β-actin and GAPDH expression by western blot. (**B**) Cell lines from **A** were treated with 100 nM or 200 nM halofuginone for 24 hours and 10 ng/μl TNF-α for 8 hours. Expression of *CXCL10* was measured by qPCR. (**C**) Cell lines were treated as in **B**. Expression of *MMP-13* was measured by qPCR.

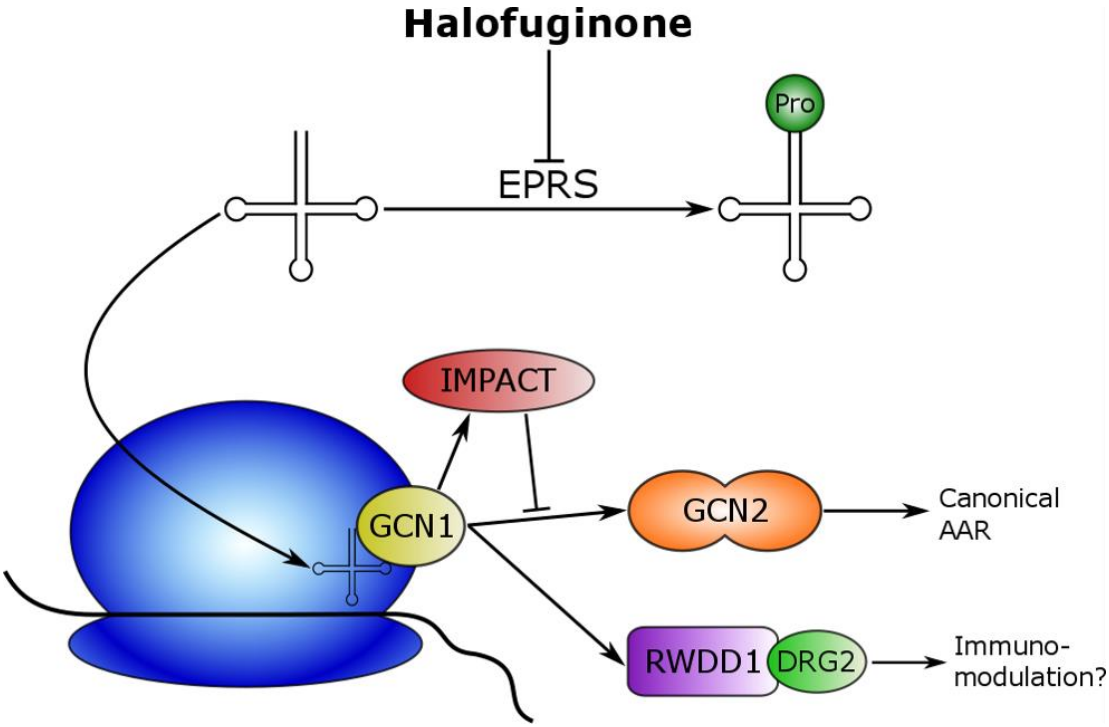

Figure 7. Proposed molecular mechanism of halofuginone. Halofuginone inhibits EPRS, preventing the charging of prolyl-tRNA. Uncharged tRNA activates GCN1 at the ribosome. GCN1 associates with GCN2 in the canonical amino acid starvation response (AAR) pathway. GCN1 also associates with RWDD1 and DRG2 in the non-canonical AAR pathway. How signaling through RWDD1 and DRG2 leads to immunomodulation remains unclear.

Chapter Three: Discussion and Perspectives

Dissecting the molecular mechanism of halofuginone offers broad insight about fundamental cellular processes such as translation. By preventing translation of proline codons, halofuginone can serve as a simple tool for studying ribosome stalling. Elongation of nascent peptides should be terminated when an uncharged prolyl-tRNA enters the A site. However, the fate of the nascent peptide remains unclear. In eukaryotic quality control pathways, the proteins Dom34 and Hbs1 are recruited to the A site when the nascent peptide is stalled in the P site and catalyze the dissociation of ribosomal subunits[110]. Then, the E3 ubiquitin ligases Lin1 and Not4 target the nascent peptide for proteasomal degradation[111]. To investigate if halofuginone acts through this pathway, proteasomal inhibitors such as MG132 or lactacystin could be added to *in vitro* translation reactions.

We identified a putative tRNA-peptide intermediate sensitive to benzonase nuclease that was generated during halofuginone treatment. It is still unclear if this complex dissociated from stalled ribosomes during *in vitro* translation or was released afterwards during SDS solubilization. Whether tRNA-peptide species can trigger any signaling pathways deserves further attention because their formation is downstream of EPRS inhibition and their elimination is caused by proline addition. If the nascent peptide, tRNA, and ribosome comprise a stable complex in the presence of halofuginone, then immunoprecipitation of N-terminal Flag-tagged nascent peptides may provide a means of ribosome isolation. These stalled ribosomes could be examined for association with AAR components such as GCN1, GCN2, RWDD1, DRG1, and DRG2.

GCN1 may play a central role in mediating the effects of halofuginone. We observed GCN1 binding to GCN2 and RWDD1, supporting its participation in both the canonical and non-

canonical AAR pathways. Furthermore, GCN1 translocated with ribosomes from the endoplasmic reticulum to the cytosol during halofuginone treatment. GCN2, RWDD1, and DRG2 were exclusively cytosolic, so halofuginone may bring GCN1 closer to its partners to promote signaling. GCN1 is proposed to transfer uncharged tRNA from the A site to GCN2[67]. To confirm this mechanism, we should look for a ~25 kDa upward band shift in GCN1 during halofuginone treatment and test its sensitivity to RNA nuclease. Since GCN1 resembles a scaffolding protein with many potential binding partners, activation by halofuginone may trigger numerous pathways. Of particular interest is interaction of GCN1 with transcription factors such as FoxP3 and PPARγ, both drivers of regulatory T cell differentiation[112,113]. In rheumatoid arthritis, FoxP3+ regulatory T cells are stimulated by synovial fibroblast-derived IL-6 and convert into Th17 cells[114]. Perhaps halofuginone can temper IL-6 inflammation, stabilize FoxP3 activity, and prevent Th17 development. These open questions motivate cell fractionation and immunofluorescence studies to identify nuclear localization of GCN1.

Our data indicate that the AAR pathways are highly conserved, reflecting their importance in regulating translation and adapting to metabolic stress. In both yeast and mammals, GCN1 associated with ribosomes and GCN2, and GCN2 formed homodimers. Whether GCN2 dimerization is also required for GCN2 and eIF2α phosphorylation in mammals has yet to be confirmed. We validated the formation of the GCN1/RWDD1/DRG2 complex in mammals which is orthologous Gcn1/Gir2/Rbg2 complex in yeast. However, due to overexpression, we were unable to determine if RWDD1 binding with DRG2 is bolstered by amino acid starvation. In yeast, the Gcn20/Gcn1 complex promotes Gcn2-dependent phosphorylation of eIF2α[76]. In *C. elegans*, the Gcn20 ortholog ABCF3 functions together with GCN1 in phosphorylating eIF2α and inducing apoptosis[115]. Whether ABCF3 interacts with

GCN1 and plays a similar role in human cells should evaluated by co-immunoprecipitation and genetic knockout studies. The wealth of literature on AAR pathways in yeast will continue to serve as an invaluable guide for unraveling the molecular mechanism of halofuginone.

Limitations

The *in vitro* translation assays were performed in a cell-free system consisting of HeLa cell lysate and accessory proteins. Ideally, the suppressive effects of halofuginone on the translation machinery should be evaluated in intact cells. However, transfection of cells with the Pro and NoPro gene blocks generated translated products before halofuginone addition, masking any apparent inhibition of translation. This could perhaps be resolved by attaching a secretory pathway signal sequence to the N-terminus of the gene blocks. Before halofuginone treatment, the cell media could be replenished to wash away any prior product. Media could later be collected and analyzed by western blot to determine if halofuginone also blocks proline translation and creates truncated products in live cells.

The resolution of Sepharose 6B column fractionation experiments could be greatly improved. We detected ribosomal markers in only two fractions and could not distinguish among polyribosomes, ribosomes, and free small and large ribosomal subunits. Higher resolution could be achieved through high-speed centrifugation of extracts through sucrose density gradients. This technique yields clean separation of 80S, 60S, and 40S ribosomes[116]. In yeast, Rbg1 preferentially associates with polyribosomes whereas Rbg2 co-fractionates with monoribosomes[80]. If DRG1 and DRG2 follows this pattern in mammalian cells, it could shed insight on the separation of signaling functions of these related proteins. Furthermore, it would

be worthwhile to test if halofuginone treatment alters the co-fractionation of ribosomal subpopulations with AAR signaling proteins.

We conducted co-immunoprecipitation experiments with overexpressed binding partners, and it is possible that such high abundance could lead to false positive interactions. Furthermore, halofuginone did not appear to significantly alter formation of GCN1/GCN2 and GCN1/RWDD1/DRG2 complexes. It is likely that halofuginone was not potent enough to regulate a meaningful proportion of the highly expressed complexes. In yeast, amino acid starvation strengthened the interaction between endogenous Gir2 and Rbg2[82]. This motivates co-immunoprecipitation or non-denaturing native gel studies of endogenous RWDD1 and DRG2 to see if their association is also modulated by amino acid availability. Likewise, the interaction between GCN1 and GCN2 as well as GCN2 dimerization should be verified endogenously with co-immunoprecipitation and non-reducing western blot respectively. Cell fractionation could elucidate whether these complexes are formed in the cytosol or at ribosomes.

Overexpression of the RWD domains of GCN2 and IMPACT failed to suppress GCN1-dependent signaling in response to halofuginone. To check if RWD domains are sufficient for GCN1 binding, co-immunoprecipitation could be performed. In yeast Gcn2 truncation studies, the pseudokinase domain increased the affinity of Gcn1 for the RWD domain[117]. Appending the GCN2 pseudokinase domain to the RWD domain may promote more efficient scavenging of available GCN1, but with additional risk of transmitting AAR signals rather than serving as a dominant negative. Overexpression of full-length IMPACT failed to inhibit phosphorylation of GCN2 and eIF2α, contrary to published studies[70]. Since we relied on transient transfection of IMPACT unlinked to the puromycin resistance gene, a population of cells lacking high IMPACT

levels may contribute to background pGCN2 signal. To resolve this complication, IMPACT should be cloned into a lentiviral transduction vector for more stable and uniform expression.

Future Research

We plan on further exploration of the role of RWDD1 and the non-canonical AAR pathway in the mechanism of halofuginone. Since the RWDD1 shRNA knockdown cell line may have reduced the effects of halofuginone on *CXCL10* and *MMP-13* expression, we will next attempt to rescue the phenotype with RWDD1 overexpression as well as create an RWDD1 knockout cell line using CRISPR-Cas9 genome editing for further study. RWDD1 is proposed to function as an adaptor protein, so downstream enzymes such as the GTPases DRG1 and DRG2 require examination through knockout, knockdown, or overexpression studies. If DRG1 and DRG2 knockdown recapitulate the effects of RWDD1 knockdown, then halofuginone is likely to act through the non-canonical AAR pathway.

Since Th17 differentiation in GCN2 knockout mice exhibited similar sensitivity to halofuginone as wild-type mice, we should repeat these experiments in RWDD1 knockout mice. If Th17 development in mice lacking RWDD1 shows insensitivity to halofuginone, then this would suggest that the non-canonical rather than the canonical AAR pathway drives Th17 development. Borrelidin treatment may demonstrate that RWDD1-dependency applies beyond proline deprivation.

Unlike the canonical AAR pathway where we can evaluate GCN2 and eIF2α phosphorylation or CHOP expression, the non-canonical AAR pathway currently lacks a clear read-out. GTPase activity could be readily measured in purified DRG1/2 with high-performance liquid chromatography or fluorescently labelled, phosphate-binding protein[118], but not in the

context of the entire cell. Increased binding to endogenous RWDD1 as is the case with yeast Gir2/Rbg1 may be a viable read-out. However, it is unclear how association with an adaptor protein stimulates GTPase activity. *In vitro* protein expression studies could determine if the presence of RWDD1 elevates the half-life of free DRG1/2. Whether halofuginone modulates the function of the associated GTPase-activating proteins or guanine nucleotide exchange factors also warrants attention.

We will continue attempts to impede GCN1 function because we expect halofuginone to act through both the canonical and non-canonical AAR pathways. GCN1 inhibition could be compared to RWDD1 inhibition or GCN2 inhibition individually to test this hypothesis. Although we were unable to create a successful GCN1 CRISPR knockout, we have established a robust shRNA knockdown. Like in yeast, loss of GCN1 reduced phosphorylation of GCN2. We hope to compare the GCN1 knockdown to the RWDD1 knockdown in future studies.

Ultimately, we hope that studies on the mechanism of halofuginone advance the development of drugs that target aminoacyl-tRNA synthetases. Halofuginone inhibits prolyl-tRNA synthetase of the malaria parasite *Plasmodium falciparum*[119], and mupirocin and furanomycin inhibit isoleucine tRNA-synthetase of methicillin-resistant *Staphylococcus aureus* (MRSA)[120]. There has been growing interest in designing novel tRNA synthetase inhibitors to address the threat of the evolution of antibiotic resistance[121]. The long term goal is to create a library of small molecules that can target each of the 20 tRNA synthetases; mimicking depletion of specific amino acids may induce different signaling pathways that could lead to diverse physiological effects. Overall, activating the amino acid starvation response pathway by drugs such as halofuginone offers a largely unexplored means to modulate the immune system and treat a wide range of diseases.

Bibliography

1. Swinney, D. C. Biochemical mechanisms of drug action: what does it take for success? *Nat Rev Drug Discov* **3**, 801–808 (2004).

2. Wilson, D. N. The A-Z of bacterial translation inhibitors. Crit. Rev. Biochem. *Mol. Biol.* **44**, 393–433 (2009).

3. Veeresham, C. Natural products derived from plants as a source of drugs. *J Adv Pharm Technol Res* **3**, 200–201 (2012).

4. Jiang, S. *et al*. Antimalarial Activities and Therapeutic Properties of Febrifugine Analogs. *Antimicrob Agents Chemother* **49**, 1169–1176 (2005).

5. Kuehl, F. A., Spencer, C. F. & Folkers, K. Alkaloids of Dichroa Febrifuga Lour. J. *Am. Chem. Soc.* **70**, 2091–2093 (1948).

6. Koepfli, J. B., Mead, J. F. & Brockman, J. A. An Alkaloid with High Antimalarial Activity from Dichroa Febrifuga. *J. Am. Chem. Soc.* **69**, 1837–1837 (1947).

7. Koepfli, J. B., Mead, J. F. & Brockman, J. A. Alkaloids of Dichroa febrifuga. I. Isolation and Degradative Studies. *J. Am. Chem. Soc.* **71**, 1048–1054 (1949).

8. Coatney, G. R., Cooper, W. C., Culwell, W. B., White, W. C. & Imboden, C. A. Studies in human malaria. XXV. Trial of febrifugine, an alkaloid obtained from Dichroa febrifuga lour., against the Chesson strain of Plasmodium vivax. *J Natl Malar Soc* **9**, 183–186 (1950).

9. Fishman, M. & Cruickshank, P. A. Febrifugine antimalarial agents. Pyridine analogs of febrifugine. *J. Med. Chem.* **13**, 155–156 (1970).

10. De Smet, P. A. The role of plant-derived drugs and herbal medicines in healthcare. *Drugs* **54**, 801–840 (1997).

11. Kikuchi, H. *et al*. Exploration of a new type of antimalarial compounds based on febrifugine. *J. Med. Chem*. **49**, 4698–4706 (2006).

12. Sen, D., Banerjee, A., Ghosh, A. K. & Chatterjee, T. K. Synthesis and antimalarial evaluation of some 4-quinazolinone derivatives based on febrifugine. *J Adv Pharm Technol Res* **1**, 401–405 (2010).

13. Takaya, Y. *et al*. New type of febrifugine analogues, bearing a quinolizidine moiety, show potent antimalarial activity against Plasmodium malaria parasite. *J. Med. Chem.* **42**, 3163–3166 (1999).

14. Kobayashi, S. *et al*. Catalytic Asymmetric Synthesis of Antimalarial Alkaloids Febrifugine and Isofebrifugine and Their Biological Activity. *J. Org. Chem*. **64**, 6833–6841 (1999).

15. Daugschies, A., Gässlein, U. & Rommel, M. Comparative efficacy of anticoccidials under the conditions of commercial broiler production and in battery trials. *Vet. Parasitol*. **76**, 163–171 (1998).

16. Klein, P. Preventive and therapeutic efficacy of halofuginone-lactate against Cryptosporidium parvum in spontaneously infected calves: a centralised, randomised, double-blind, placebo-controlled study. *Vet. J.* **177**, 429–431 (2008).

17. Derbyshire, E. R., Mazitschek, R. & Clardy, J. Characterization of Plasmodium liver stage inhibition by halofuginone. *ChemMedChem* **7**, 844–849 (2012).

18. Geary, T. G., Divo, A. A. & Jensen, J. B. Stage specific actions of antimalarial drugs on Plasmodium falciparum in culture. *Am. J. Trop. Med. Hyg.* **40**, 240–244 (1989).
19. Pines, M. & Spector, I. Halofuginone - the multifaceted molecule. *Molecules* **20**, 573–594 (2015).

20. Spector, I. *et al*. Inhibition of pancreatic stellate cell activation by halofuginone prevents pancreatic xenograft tumor development. *Pancreas* **39**, 1008–1015 (2010).

21. Elkin, M. *et al*. Inhibition of bladder carcinoma angiogenesis, stromal support, and tumor growth by halofuginone. *Cancer Res.* **59**, 4111–4118 (1999).

22. Gavish, Z. *et al*. Growth inhibition of prostate cancer xenografts by halofuginone. *Prostate* **51**, 73–83 (2002).

23. Pinthus, J. H. *et al*. Inhibition of Wilms tumor xenograft progression by halofuginone is accompanied by activation of WT-1 gene expression. *J. Urol.* **174**, 1527–1531 (2005).

24. Van Kempen, L. C. L. T. *et al*. Type I collagen expression contributes to angiogenesis and the development of deeply invasive cutaneous melanoma. *Int. J. Cancer* **122**, 1019–1029 (2008).

25. Chen, G. *et al*. Halofuginone inhibits colorectal cancer growth through suppression of Akt/mTORC1 signaling and glucose metabolism. *Oncotarget* **6**, 24148–24162 (2015).

26. Gross, D. J. *et al*. Treatment with halofuginone results in marked growth inhibition of a von Hippel-Lindau pheochromocytoma *in vivo*. *Clin. Cancer Res*. **9**, 3788–3793 (2003).

27. Juárez, P. *et al*. Halofuginone inhibits the establishment and progression of melanoma bone metastases. *Cancer Res.* **72**, 6247–6256 (2012).

28. Taras, D. *et al*. Halofuginone suppresses the lung metastasis of chemically induced hepatocellular carcinoma in rats through MMP inhibition. *Neoplasia* **8**, 312–318 (2006).

29. Jin, M. L., Park, S. Y., Kim, Y. H., Park, G. & Lee, S. J. Halofuginone induces the apoptosis of breast cancer cells and inhibits migration via downregulation of matrix metalloproteinase-9. *Int. J. Oncol*. **44**, 309–318 (2014).

30. Abramovitch, R., Dafni, H., Neeman, M., Nagler, A. & Pines, M. Inhibition of neovascularization and tumor growth, and facilitation of wound repair, by halofuginone, an inhibitor of collagen type I synthesis. *Neoplasia* **1**, 321–329 (1999).

31. Sheffer, Y. *et al*. Inhibition of fibroblast to myofibroblast transition by halofuginone contributes to the chemotherapy-mediated antitumoral effect. *Mol. Cancer Ther.* **6**, 570–577 (2007).

32. Halevy, O., Nagler, A., Levi-Schaffer, F., Genina, O. & Pines, M. Inhibition of collagen type I synthesis by skin fibroblasts of graft versus host disease and scleroderma patients: effect of halofuginone. *Biochem. Pharmacol.* **52**, 1057–1063 (1996).

33. Levi-Schaffer, F., Nagler, A., Slavin, S., Knopov, V. & Pines, M. Inhibition of collagen synthesis and changes in skin morphology in murine graft-versus-host disease and tight skin mice: effect of halofuginone. *J. Invest. Dermatol.* **106**, 84–88 (1996).

34. Zion, O. *et al*. Inhibition of transforming growth factor beta signaling by halofuginone as a modality for pancreas fibrosis prevention. *Pancreas* **38**, 427–435 (2009).

35. Huebner, K. D., Jassal, D. S., Halevy, O., Pines, M. & Anderson, J. E. Functional resolution of fibrosis in mdx mouse dystrophic heart and skeletal muscle by halofuginone. *Am. J. Physiol. Heart Circ. Physiol.* **294**, 1550–1561 (2008).

36. Spira, G. *et al*. Halofuginone, a collagen type I inhibitor improves liver regeneration in cirrhotic rats. *J. Hepatol*. **37**, 331–339 (2002).

37. Pines, M. *et al*. Reduction in dermal fibrosis in the tight-skin (Tsk) mouse after local application of halofuginone. *Biochem. Pharmacol.* **62**, 1221–1227 (2001).

38. Popov, Y. *et al*. Halofuginone induces matrix metalloproteinases in rat hepatic stellate cells via activation of p38 and NFkappaB. *J. Biol. Chem*. **281**, 15090–15098 (2006).

39. Zcharia, E. *et al*. Inhibition of matrix metalloproteinase-2 by halofuginone is mediated by the Egr1 transcription factor. *Anticancer Drugs* **23**, 1022–1031 (2012).

40. Bruck, R. *et al*. Halofuginone to prevent and treat thioacetamide-induced liver fibrosis in rats. *Hepatology* **33**, 379–386 (2001).

41. Roffe, S., Hagai, Y., Pines, M. & Halevy, O. Halofuginone inhibits Smad3 phosphorylation via the PI3K/Akt and MAPK/ERK pathways in muscle cells: effect on myotube fusion. *Exp. Cell Res.* **316**, 1061–1069 (2010).

42. Xavier, S. *et al*. Amelioration of radiation-induced fibrosis: inhibition of transforming growth factor-beta signaling by halofuginone. *J. Biol. Chem*. **279**, 15167–15176 (2004).

43. Verrecchia, F. & Mauviel, A. Transforming growth factor-beta and fibrosis. *World J. Gastroenterol.* **13**, 3056–3062 (2007).

44. Saito, S., Nakashima, A., Shima, T. & Ito, M. Th1/Th2/Th17 and Regulatory T-Cell Paradigm in Pregnancy. *American Journal of Reproductive Immunology* **63**, 601–610 (2010).

45. Korn, T., Bettelli, E., Oukka, M. & Kuchroo, V. K. IL-17 and Th17 Cells. *Annu. Rev. Immunol.* **27**, 485–517 (2009).

46. Noack, M. & Miossec, P. Th17 and regulatory T cell balance in autoimmune and inflammatory diseases. *Autoimmunity Reviews* **13**, 668–677 (2014).

47. Sundrud, M. S. *et al*. Halofuginone inhibits TH17 cell differentiation by activating the amino acid starvation response. *Science* **324**, 1334–1338 (2009).

48. Pietrella, D. *et al*. Th17 Cells and IL-17 in Protective Immunity to Vaginal Candidiasis. *PLOS ONE* **6**, e22770 (2011).

49. Deselm, C. J., Zou, W. & Teitelbaum, S. L. Halofuginone prevents estrogen-deficient osteoporosis in mice. *J. Cell. Biochem*. **113**, 3086–3092 (2012).

50. Park, M.-K. *et al.* Halofuginone ameliorates autoimmune arthritis in mice by regulating the balance between Th17 and Treg cells and inhibiting osteoclastogenesis. *Arthritis & Rheumatology* **66**, 1195–1207 (2014).

51. Cui, Z. *et al*. Halofuginone attenuates osteoarthritis by inhibition of TGF-β activity and H-type vessel formation in subchondral bone. *Ann Rheum Dis*, 2015–207923 (2015).

52. Oishi, H. *et al*. Halofuginone Treatment reduces interleukin-17A and ameliorates features of chronic lung allograft dysfunction in a mouse orthotopic lung transplant model. *J. Heart Lung Transplant*. (2015).

53. Keller, T. L. *et al*. Halofuginone and other febrifugine derivatives inhibit prolyl-tRNA synthetase. *Nat. Chem. Biol.* **8**, 311–317 (2012).

54. Laplante, M. & Sabatini, D. M. mTOR signaling in growth control and disease. *Cell* **149**, 274–293 (2012).

55. Mihaylova, M. M. & Shaw, R. J. The AMP-activated protein kinase (AMPK) signaling pathway coordinates cell growth, autophagy, & metabolism. *Nat. Cell Biol.* **13**, 1016–1023 (2011).

56. Sancak, Y. *et al*. The Rag GTPases bind raptor and mediate amino acid signaling to mTORC1. *Science* **320**, 1496–1501 (2008).

57. Sood, R., Porter, A. C., Olsen, D., Cavener, D. R. & Wek, R. C. A Mammalian Homologue of GCN2 Protein Kinase Important for Translational Control by Phosphorylation of Eukaryotic Initiation Factor-2α. *Genetics* **154**, 787–801 (2000).

58. Castilho, B. A. *et al*. Keeping the eIF2 alpha kinase Gcn2 in check. *Biochimica et Biophysica Acta (BBA) - Molecular Cell Research* **1843**, 1948–1968 (2014).

59. Clemens, M. J. Initiation factor eIF2 alpha phosphorylation in stress responses and apoptosis. *Prog. Mol. Subcell. Biol.* **27**, 57–89 (2001).

60. Richter, J. D. & Sonenberg, N. Regulation of cap-dependent translation by eIF4E inhibitory proteins. *Nature* **433**, 477–480 (2005).

61. Averous, J. *et al*. Induction of CHOP Expression by Amino Acid Limitation Requires Both ATF4 Expression and ATF2 Phosphorylation. *J. Biol. Chem.* **279**, 5288–5297 (2004).

62. Chikka, M. R., McCabe, D. D., Tyra, H. M. & Rutkowski, D. T. C/EBP homologous protein (CHOP) contributes to suppression of metabolic genes during endoplasmic reticulum stress in the liver. *J. Biol. Chem.* **288**, 4405–4415 (2013).

63. Nishitoh, H. CHOP is a multifunctional transcription factor in the ER stress response. *J. Biochem*. *151*, 217–219 (2012).

64. B'chir, W. *et al*. The eIF2α/ATF4 pathway is essential for stress-induced autophagy gene expression. *Nucl. Acids Res.* **563** (2013).

65. Ye, J. *et al*. The GCN2-ATF4 pathway is critical for tumour cell survival and proliferation in response to nutrient deprivation. *EMBO J* **29**, 2082–2096 (2010).

66. Örd, D., Meerits, K. & Örd, T. TRB3 protects cells against the growth inhibitory and cytotoxic effect of ATF4. *Experimental Cell Research* **313**, 3556–3567 (2007).

67. Marton, M. J., Vazquez de Aldana, C. R., Qiu, H., Chakraburtty, K. & Hinnebusch, A. G. Evidence that GCN1 and GCN20, translational regulators of GCN4, function on elongating ribosomes in activation of eIF2alpha kinase GCN2. *Mol. Cell. Biol.* **17**, 4474–4489 (1997).

68. Lee, S. J., Swanson, M. J. & Sattlegger, E. Gcn1 contacts the small ribosomal protein Rps10, which is required for full activation of the protein kinase Gcn2. *Biochem. J.* **466**, 547–559 (2015).

69. Nameki, N. *et al*. Solution structure of the RWD domain of the mouse GCN2 protein. *Protein Sci.* **13**, 2089–2100 (2004).

70. Cambiaghi, T. D. *et al*. Evolutionarily conserved IMPACT impairs various stress responses that require GCN1 for activating the eIF2 kinase GCN2. *Biochem. Biophys. Res. Commun.* **443**, 592–597 (2014).

71. Averous, J. *et al*. Induction of CHOP Expression by Amino Acid Limitation Requires Both ATF4 Expression and ATF2 Phosphorylation. *J. Biol. Chem.* **279**, 5288–5297 (2004).

72. Huttlin, E. L. *et al*. The BioPlex Network: A Systematic Exploration of the Human Interactome. *Cell* **162**, 425–440 (2015).

73. Rudra, D. *et al.* Transcription factor Foxp3 and its protein partners form a complex regulatory network. *Nat. Immunol.* **13**, 1010–1019 (2012).

74. Schubert, L. A., Jeffery, E., Zhang, Y., Ramsdell, F. & Ziegler, S. F. Scurfin (FOXP3) acts as a repressor of transcription and regulates T cell activation. *J. Biol. Chem.* **276**, 37672–37679 (2001).

75. Freeman, G. J. *et al*. Engagement of the PD-1 immunoinhibitory receptor by a novel B7 family member leads to negative regulation of lymphocyte activation. *J. Exp. Med.* **192**, 1027–1034 (2000).

76. Garcia-Barrio, M., Dong, J., Ufano, S. & Hinnebusch, A. G. Association of GCN1-GCN20 regulatory complex with the N-terminus of eIF2alpha kinase GCN2 is required for GCN2 activation. *EMBO J.* **19**, 1887–1899 (2000).

77. Sattlegger, E. & Hinnebusch, A. G. Separate domains in GCN1 for binding protein kinase GCN2 and ribosomes are required for GCN2 activation in amino acid-starved cells. *EMBO J.* **19**, 6622–6633 (2000).

78. Marton, M. J., Crouch, D. & Hinnebusch, A. G. GCN1, a translational activator of GCN4 in Saccharomyces cerevisiae, is required for phosphorylation of eukaryotic translation initiation factor 2 by protein kinase GCN2. *Mol. Cell. Biol.* **13**, 3541–3556 (1993).

79. Sattlegger, E. & Hinnebusch, A. G. Polyribosome binding by GCN1 is required for full activation of eukaryotic translation initiation factor 2{alpha} kinase GCN2 during amino acid starvation. *J. Biol. Chem.* **280**, 16514–16521 (2005).

80. Wout, P. K., Sattlegger, E., Sullivan, S. M. & Maddock, J. R. *Saccharomyces cerevisiae* Rbg1 protein and its binding partner Gir2 interact on Polyribosomes with Gcn1. *Eukaryotic Cell* **8**, 1061–1071 (2009).

81. Francis, S. M., Gas, M.-E., Daugeron, M.-C., Bravo, J. & Séraphin, B. Rbg1–Tma46 dimer structure reveals new functional domains and their role in polysome recruitment. *Nucleic Acids Res* **40**, 11100–11114 (2012).

82. Ishikawa, K., Ito, K., Inoue, J. & Semba, K. Cell growth control by stable Rbg2/Gir2 complex formation under amino acid starvation. *Genes Cells* **18**, 859–872 (2013).

83. Murguía, J. R. & Serrano, R. New functions of protein kinase Gcn2 in yeast and mammals. *IUBMB Life* **64**, 971–974 (2012).

84. Kang, N. *et al*. Identification and Characterization of a Novel Thymus Aging Related Protein Rwdd1. *Cell Mol Immunol* **5**, 279–285 (2008).

85. Rolland, T. *et al*. A proteome-scale map of the human interactome network. *Cell* **159**, 1212–1226 (2014).

86. Wan, C. *et al*. Panorama of ancient metazoan macromolecular complexes. *Nature* **525**, 339–344 (2015).

87. Pérez-Arellano, I., Spínola-Amilibia, M. & Bravo, J. Human Drg1 is a potassium-dependent GTPase enhanced by Lerepo4. *FEBS J.* **280**, 3647–3657 (2013).

88. Ishikawa, K., Akiyama, T., Ito, K., Semba, K. & Inoue, J. Independent stabilizations of polysomal Drg1/Dfrp1 complex and non-polysomal Drg2/Dfrp2 complex in mammalian cells. *Biochemical and Biophysical Research Communications* **390**, 552–556 (2009).

89. Stark, C. *et al*. BioGRID: a general repository for interaction datasets. *Nucleic Acids Res.* **34**, D535–539 (2006).

90. Mani, M. *et al*. Developmentally regulated GTP-binding protein 2 coordinates Rab5 activity and transferrin recycling. *Mol. Biol. Cell* **27**, 334–348 (2016).

91. Ke, K. *et al*. Overexpression of developmentally regulated GTP-binding protein-2 increases bone loss. *Am. J. Physiol. Endocrinol. Metab*. **304**, E703–710 (2013).

92. Ko, M. S. *et al.* Developmentally regulated GTP-binding protein 2 ameliorates EAE by suppressing the development of TH17 cells. *Clin. Immunol*. **150**, 225–235 (2014).

93. Chon, S. Y., Hassanain, H. H. & Gupta, S. L. Cooperative role of interferon regulatory factor 1 and p91 (STAT1) response elements in interferon-gamma-inducible expression of human indoleamine 2,3-dioxygenase gene. *J. Biol. Chem.* **271**, 17247–17252 (1996).

94. Currier, A. R. *et al*. Tumor necrosis factor-alpha and lipopolysaccharide enhance interferon-induced antichlamydial indoleamine dioxygenase activity independently. J. *Interferon Cytokine Res.* **20**, 369–376 (2000).

95. Munn, D. H. Indoleamine 2,3-dioxygenase, Tregs and cancer. *Curr. Med. Chem.* **18**, 2240–2246 (2011).

96. Shinde, R., Chaudhary, K., Shimoda, M., Pacholczyk, G. & McGaha, T. Indoleamine 2,3-dioxygenase inhibits B cell immune response to T independent antigens. *J. Immunol*. **192**, 127.11–127.11 (2014).

97. Fallarino, F. *et al*. T cell apoptosis by kynurenines. *Adv. Exp. Med. Biol.* **527**, 183–190 (2003).

98. Ishiguro, I., Naito, J., Saito, K. & Nagamura, Y. Skin L-tryptophan-2,3-dioxygenase and rat hair growth. *FEBS Lett*. **329**, 178–182 (1993).

99. Miller, C. L. *et al*. Expression of the kynurenine pathway enzyme tryptophan 2,3-dioxygenase is increased in the frontal cortex of individuals with schizophrenia. *Neurobiol. Dis*. **15**, 618–629 (2004).

100. Schmidt, S. K. *et al*. Antimicrobial and immunoregulatory properties of human tryptophan 2,3-dioxygenase. *Eur. J. Immunol*. **39,** 2755–2764 (2009).

101. Zea, A. H. *et al*. L-Arginine modulates CD3zeta expression and T cell function in activated human T lymphocytes. *Cell. Immunol*. **232**, 21–31 (2004).

102. Vig, M. *et al*. Inducible nitric oxide synthase in T cells regulates T cell death and immune memory. *J. Clin. Invest.* **113**, 1734–1742 (2004).

103. Yang, J. *et al*. T cell–derived inducible nitric oxide synthase switches off Th17 cell differentiation. *J. Exp. Med.* **210**, 1447–1462 (2013).

104. McGaha, T. L. *et al*. Amino acid catabolism: a pivotal regulator of innate and adaptive immunity. *Immunol Rev* **249**, 135–157 (2012).

105. Munn, D. H. *et al*. GCN2 kinase in T cells mediates proliferative arrest and anergy induction in response to indoleamine 2,3-dioxygenase. *Immunity* **22**, 633–642 (2005).

106. Qiu, H., Garcia-Barrio, M. T. & Hinnebusch, A. G. Dimerization by translation initiation factor 2 kinase GCN2 is mediated by interactions in the C-terminal ribosome-binding region and the protein kinase domain. *Mol. Cell. Biol*. **18**, 2697–2711 (1998).

107. Qiu, H., Dong, J., Hu, C., Francklyn, C. S. & Hinnebusch, A. G. The tRNA-binding moiety in GCN2 contains a dimerization domain that interacts with the kinase domain and is required for tRNA binding and kinase activation. *EMBO J* **20**, 1425–1438 (2001).

108. Wang, T. *et al*. Identification and characterization of essential genes in the human genome. *Science* **350**, 1096–1101 (2015).

109. D'Aniello, C. *et al*. A novel autoregulatory loop between the Gcn2-Atf4 pathway and L-Proline metabolism controls stem cell identity. *Cell Death Differ* **22**, 1094–1105 (2015).

110. Tsuboi, T. *et al*. Dom34:hbs1 plays a general role in quality-control systems by dissociation of a stalled ribosome at the 3' end of aberrant mRNA. *Mol. Cell* **46**, 518–529 (2012).

111. Bengtson, M. H. & Joazeiro, C. A. P. Role of a ribosome-associated E3 ubiquitin ligase in protein quality control. *Nature* **467**, 470–473 (2010).

112. Sakaguchi, S., Miyara, M., Costantino, C. M. & Hafler, D. A. FOXP3+ regulatory T cells in the human immune system. *Nat Rev Immunol* **10**, 490–500 (2010).

113. Cipolletta, D. *et al*. PPAR-γ is a major driver of the accumulation and phenotype of adipose tissue Treg cells. *Nature* **486**, 549–553 (2012).

114. Komatsu, N. et al. Pathogenic conversion of Foxp3+ T cells into TH17 cells in autoimmune arthritis. *Nat. Med.* **20**, 62–68 (2014).

115. Hirose, T. & Horvitz, H. R. The translational regulators GCN-1 and ABCF-3 act together to promote apoptosis in C. elegans. *PLoS Genet*. **10**, e1004512 (2014).

116. Esposito, A. M. *et al*. Eukaryotic Polyribosome Profile Analysis. *J Vis Exp* **40** (2010).

117. Lageix, S., Rothenburg, S., Dever, T. E. & Hinnebusch, A. G. Enhanced interaction between pseudokinase and kinase domains in Gcn2 stimulates eIF2α phosphorylation in starved cells. *PLoS Genet*. **10**, e1004326 (2014).

118. Shutes, A. & Der, C. J. Real-time in vitro measurement of GTP hydrolysis. *Methods* **37**, 183–189 (2005).

119. Herman, J. D. *et al*. The cytoplasmic prolyl-tRNA synthetase of the malaria parasite is a dual-stage target of febrifugine and its analogs. *Sci Transl Med* **7**, 288ra77 (2015).

120. Kim, S., Lee, S. W., Choi, E.-C. & Choi, S. Y. Aminoacyl-tRNA synthetases and their inhibitors as a novel family of antibiotics. *Appl Microbiol Biotechnol* **61**, 278–288 (2003).

121. Lv, P.-C. & Zhu, H.-L. Aminoacyl-tRNA synthetase inhibitors as potent antibacterials. *Curr. Med. Chem*. **19**, 3550–3563 (2012).